Dynamics of Atmospheres and Oceans 71 (2015) 56–82

Contents lists available at ScienceDirect

Dynamics of Atmospheres and Oceans

journal homepage: www.elsevier.com/locate/dynatmoce

Storm surges in the Mediterranean Sea: Variability and trends under future climatic conditions

Yannis S. Androulidakis, Katerina D. Kombiadou, Christos V. Makris, Vassilis N. Baltikas, Yannis N. Krestenitis*

Laboratory of Maritime Engineering and Maritime Works, Civil Engineering Department, Aristotle University of Thessaloniki, 54124 Thessaloniki, Greece

ARTICLE INFO

Article history:
Received 6 October 2014
Received in revised form 20 May 2015
Accepted 1 June 2015
Available online 3 June 2015

Keywords:
Storm surge
Climate change
Mediterranean sea
Hydrodynamic modeling

ABSTRACT

The trends of storm surge extremes in the Mediterranean Sea for a period of 150 years (1951–2100) are explored, using a high-resolution storm surge model. Numerical simulations are forced by the output of regional climate simulations with RegCM3, which uses IPCC's historical data on greenhouse gasses emissions for the (past) period 1951–2000, and IPCC's A1B climate scenario for the (future) period 2001–2100. Comparisons between observations and modeling results show good agreement and confirm the ability of our model to estimate the response of the sea surface to future climatic conditions. We investigate the future trends, the variability and frequency of local extremes and the main forcing mechanisms that can induce strong surges in the Mediterranean region. Our results support that there is a general decreasing trend in storminess under the considered climate scenario, mostly related to the frequency of local peaks and the duration and spatial coverage of the storm surges. The northward shift in the location of storm tracks is a possible reason for this storminess attenuation, especially over areas where the main driving factor of extreme events is the inverted barometer effect. However, the magnitudes of sea surface elevation extremes may increase in several Mediterranean sub-regions, *i.e.*, Southern Adriatic, Balearic and Tyrrhenian Seas, during the 21st century. There are clear distinctions in the contributions of winds and pressure fields to the sea level height for various regions of the Mediterranean Sea, as well as on the seasonal variability of extreme values; the Aegean and Adriatic Seas are characteristic examples, where high surges are predicted to be mainly induced by low pressure systems and favorable winds, respectively.

1. Introduction

Low-elevation areas along the Mediterranean coastline are at high risk in cases of extreme storm surge events; extreme storms may induce significant direct (*e.g.* flooding, coastal erosion, damage to property) and indirect (*e.g.* salt intrusion, land subsidence, water supply contamination, vegetation destruction) impacts to the coastal zone (White, 1974). The existence of numerous coastal cities, river deltas, islands, low land elevation coastal areas and topographically complicated regions (*e.g.*

* Corresponding author at: Division of Hydraulics and Environmental Engineering, Civil Engineering Department, Aristotle University of Thessaloniki, University campus, 54124 Thessaloniki, Greece. Fax: +30 231 0995649.
E-mail addresses: iandroul@civil.auth.gr (Y.S. Androulidakis), kobiadou@civil.auth.gr (K.D. Kombiadou), cmakris@civil.auth.gr (C.V. Makris), vmpaltik@civil.auth.gr (V.N. Baltikas), ynkrest@civil.auth.gr (Y.N. Krestenitis).

http://dx.doi.org/10.1016/j.dynatmoce.2015.06.001
0377-0265/$ – see front matter

Adriatic Sea, Aegean Archipelago) over the Mediterranean coastal zone, support the need to consider possible climate change impacts in coastal planning. Nicholls and Hoozemans (1996) argued that coastal management in the Mediterranean Sea needs to address long-term problems and, especially, the impact of climate change on the sea level elevation. Although the tidal signal is an important sea level height factor, the Mediterranean basin's sea level extremes are mainly related to storm surges rather than to the combination of tides and surges (Marcos et al., 2009). The aim of the present paper is to investigate the interannual, seasonal and spatial variability of storm surges in the Mediterranean for the 21st century under specific climatic conditions (A1B scenario, IPCC, 2001), to assess the frequencies of surge maxima and to identify the main driving mechanisms of the latter, in different regional seas.

Storm surges may have significant differences between the various Mediterranean regions, due to the topography of each area and the storm characteristics. There is a high correlation between the surges over the western and central Mediterranean and the North Atlantic Oscillation (Marcos et al., 2009), while its relation with surges in the eastern Mediterranean is also significant but weaker due to the distance from the atmospheric (pressure) action centers. Storm surge events in the Aegean Sea generally exhibit low magnitude and occurrence frequencies of extreme events (Krestenitis et al., 2011). Tsimplis et al. (2009a) investigated the relationship between extreme sea levels and estimated return periods over a temporal span of 14 years, based on measurements from tide-gauges of the Southern European Seas (Iberian, Atlantic and Mediterranean stations); they found significant differences between the various sub-regions. Tsimplis and Blackman (1997) also analyzed tide-gauge data to estimate the return periods of extreme sea levels in the Aegean and Ionian Seas over a period of eight years. Satellite altimetry data for the 1993–2000 period (Tsimplis et al., 2009b) and numerical simulations for the 2000–2004 period (Krestenitis et al., 2011), showed that the increasing gradient of the sea level trend is steeper over the eastern than the western Mediterranean coasts. Significant spatial variability was identified in observations from all seasons (Tsimplis and Shaw, 2010). Regarding the North (N) Adriatic basin, its shape determines unique sea surface dynamics with seiches, surges, astronomical tides, and the long fetch of strong southeasterly winds (Sirocco) that may favor intense storm surge conditions (Lionello et al., 2012a). According to Marcos et al. (2009), the tidal effects may add up to 30 cm in the N. Adriatic coastal region. Another region with intense atmospheric cyclogenesis in the Mediterranean is the Levantine basin (Campins et al., 2011).

The seasonal distribution of sea storms over the Mediterranean region presented significant changes in the last centuries. A change in the seasonal wind patterns may bring storm frequency changes and alter the sea level variations due to meteorological conditions (Camuffo et al., 2000). Such changes in sea storm frequency were strongly associated with tremendous floods in the Spanish Mediterranean coastal zone in the late 16th century, late 17th century, and mid 19th century. Mediterranean surges have a clear seasonal distribution with high positive surges, occurring mostly in winter (Marcos et al., 2011). At the same time, Marcos et al. (2011) also showed an increase in the number of events with higher atmospheric pressure over southern Europe during the 21st century, which are, in turn, linked to fewer number of cyclones over the Mediterranean and, therefore, to a decrease in the number of positive storm surges.

Several global and regional studies showed that changes in atmospheric storminess, predicted for the 21st century, may induce respective alterations to water level heights. According to Giorgi (2006), the Mediterranean is a 'hot spot' for climate change. Bengtsson et al. (2006) investigated extensively the storm track changes over the global ocean under the A1B future climatic scenario, used in the current study. Lowe and Gregory (2005) based their work on global climate simulations for 50 or 100 years into the future, and argued that the best practice is to predict the number of events that may exceed a specific height in a fixed length of time. However, global climate models are not sufficient to represent the complexity of the geomorphology of the Mediterranean region (Gualdi et al., 2013). Regional, high spatial resolution models, forced by high resolution atmospheric fields, are required to properly reproduce regional sea level variability processes (Calafat et al., 2012). Recent downscaling techniques improved the simulated trends of atmospheric and oceanic parameters (Somot et al., 2008; Gualdi et al., 2013) over the Mediterranean Sea, by incorporating the small-scale features of the basin. Jordà et al. (2012) investigated the atmospheric contribution to the Mediterranean Sea level variability under three different climate change scenarios (B1, A1B and A2); they found decreasing trends over the western and eastern parts of the basin that range between -0.03 ± 0.03 mm/year and -0.04 ± 0.03 mm/year, -0.16 ± 0.05 mm/year and -0.18 ± 0.04 mm/year and -0.22 ± 0.04 mm/year and -0.25 ± 0.04 mm/year for scenarios B1, A1B and A2, respectively. Similarly, Šepić et al. (2012) found that the sea level trends induced by atmospheric pressure and wind are negative in future climate projections for the medium-emission (A1B) scenario in the Mediterranean Sea. This finding agrees with the analysis of Conte and Lionello (2013), who showed that the climate change, under A1B scenario, may bring a likely attenuation of storminess for the period 1951–2050. However, a localized and/or temporal increase of the mean sea level and land subsidence might still increase the hazard posed by coastal floods due to storm surges. The impact of climate change on the storminess of the N. Adriatic Sea has been examined extensively in numerous recent studies (*e.g.* Lionello, 2005; Nicholls, 2006; Lionello et al., 2003, 2012a,b). Bondesan et al. (1995) showed that, even in the absence of new human activities triggering land-subsidence processes, the additional loss in land level by the year 2100 is expected to vary between 0.5 and 1.5 m in certain areas of the northwestern Adriatic coastal region.

In the present work, we seek to explore the trends of sea level extremes due to atmospheric conditions for a period of 150 years, under a climate scenario with highly increasing concentrations of atmospheric greenhouse gases. The climate change scenario used in our study is A1B, one of the 35 Special Report on Emission Scenarios (SRES) of the Intergovernmental Panel on Climate Change (IPCC, 2001). The A1B emission scenario is applied on the 3rd version of the Regional Climate Model (RegCM3; Pal et al., 2007). The RegCM3 model's output, in turn, forces a hydrodynamic storm surge model, namely

Mediterranean Climate Surge Model (MeCSM), for a period of 150 years, starting from 1951. Evaluation of the MeCSM model against available *in situ* measurements showed that the simulation from 1951 until today (control run, presented in Section 2.1) can efficiently reproduce spatial and temporal distribution of the Sea Level Height (SLH) extremes. We also investigated the evolution of seasonal variability and the contribution of each atmospheric factor (pressure and wind) on the general trend of SLH distribution, along the Mediterranean coastline and over the Mediterranean sub-basins (*e.g.* Aegean Sea, Adriatic Sea). We divided the study period into two main sub-periods: the *Past Period* (1951–2000) and the *Future Period* (2001–2100) and compared them in order to detect changes on the maximum SLHs and on their occurrence frequencies over the various Mediterranean sub-regions. Both periods are parts of the continuous 150- year climatic simulation, forced by the RegCM3 implementation in the Mediterranean Sea. Moreover, specific periods and regions of increased coastal vulnerability due to high frequencies of sea level extremes were detected.

Following this introductory section, the methodology of the study is presented in Section 2, including a detailed description of the numerical simulations, the study domain, the forcing input and the available *in situ* observations. The evaluation of the model is presented in Section 3. Section 4 includes the main results regarding the SLH evolution and variability in the Mediterranean coastal zone and broader sub- basins of the region. The discussion about the general SLH trends and the distribution of extremes along the coastal zone during the entire 150-year simulation period is presented in Section 5, followed by a summary of the main conclusions (Section 6).

2. Methodology

2.1. The atmospheric climate model

The Regional Climate Model (RegCM) was developed by the International Centre for Theoretical Physics (ICTP) in Trieste, based on the Mesoscale Model version 4 (MM4) from the National Center for Atmospheric Research-Pennsylvania State University (NCAR-PSU). RegCM is a finite-differences atmospheric model, with hydrostatic balance and sigma vertical coordinates, which accounts for the sub-grid scale variability of clouds (Giorgi et al., 1993a; Giorgi et al., 1993b; Pal et al., 2000). RegCM has been used extensively for climate simulations, to investigate past and/or future evolution of several atmospheric parameters such as rainfall, air temperature and winds over smaller (*i.e.* Sahara, Caribbean) or broader (*i.e.* Africa, Indian Ocean, Asia) regions (*i.e.* Seth et al., 2007; Davis et al., 2009; Sylla et al., 2010; Torma et al., 2011; Ozturk et al., 2012). Future changes on the climatology of cyclones in Europe (Lionello et al., 2008a) and specifically over the Mediterranean Sea (Lionello and Giorgi, 2007), under different climate scenarios, have also been investigated with RegCM simulations. Coupling of RegCM with a wave model was also used to study the climate changes on the wind–wave interactions in the Mediterranean Sea in the end of the 21st century (Lionello et al., 2008b).

The numerical climate simulations were developed by the Department of Meteorology and Climatology of Aristotle University of Thessaloniki, in the framework of the THALES research programme and namely the project entitled "Estimating the effects of Climate Change on SEA level and WAVe climate of the Greek seas, coastal Vulnerability and Safety of coastal and marine structures" (CCSEAWAVS, www.thalis-ccseawavs.web.auth.gr); the goal of the project was to assess the impacts climate change on the marine climate, waves and storm surges of the Mediterranean Sea, focusing especially on the Greek seas. The A1B emission scenario is based on the assumption that all the energy sources will be equally used, and is characterized as a pessimistic scenario, with the CO_2 concentrations reaching up to 815 ppm until the end of 21st century (IPCC, 2001). Generally, the A1B scenario belongs to the A1 category, which describes a future of very rapid economic growth, highly populated with new and more efficient technologies. Under the A1B emission conditions, wind and Sea Level Pressure (SLP) fields were simulated for the entire Mediterranean region, with spatial horizontal resolution of 25×25 km. The atmospheric model grid has 192×108 horizontal points and is divided to 18 vertical levels (Table 1). The simulation covers the period from 1/1/1951 to 31/12/2100 with a 60 s time step. Tegoulias et al. (2013), Velikou et al. (2014) and Vagenas et al. (2014) presented extensive information and validation with *in situ* data regarding the effectiveness of the RegCM3 implementation to investigate climate changes over Europe. RegCM3 uses historical data (20C3M) for the period

Table 1
Basic parameterizations of RegCM3 implementation in the Mediterranean Sea.

Parameterization	RegCM3
Driving field	ECHAM5
Control run forcing (1951–2000)	20C3M
Climatic scenario forcing (2001–2100)	A1B (IPCC, 2001)
Number of grid points	192×108
Number of vertical levels	18
Integration time	Jan 1, 1951–Dec 31, 2100
Time step	60 s
Terrain and land use resolution	10 min
Cumulus scheme	Grell (1993)
Convective closure scheme	Fritsch and Chappell (1980)
Planetary boundary layer scheme	Holtslag and Moeng (1991)

1951–2000 (*Past Period*); these data archive greenhouse gasses emissions increase as observed through the 20th century (IPCC, 2001). For the future projections (2001–2100) the regional model uses SRES emission scenario A1B, as described above. Therefore, the *Past Period* refers to a control climatic run and the *Future Period* corresponds to simulations with the future climatic scenario (A1B). This distinction between the *Past* and *Future Periods* is used throughout the present paper, to express the control and scenario-based climatic simulations, respectively.

The RegCM3 simulations provided the atmospheric forcing input of the hydrodynamic storm surge model (see Section 2.2), for the entire 150-year simulation period. Further elaboration on the description and results of the atmospheric RegCM3 simulations is considered beyond the scope of the study.

2.2. The storm surge model

The Mediterranean Climate Surge Model (MeCSM) is based on the Aristotle University of Thessaloniki Storm Surge Model (AUTSSM; De Vries et al., 1995; Krestenitis et al., 2011; Trifonova et al., 2012; Villatoro et al., 2014). MeCSM is a two-dimensional hydrodynamic model that solves the depth-averaged shallow water equations and is used to predict the sea level for the entire Mediterranean basin on a $1/10^\circ \times 1/10^\circ$ horizontal grid. The 6-hourly atmospheric forcing, namely the winds at 10 m elevation from mean sea level and the SLP fields, are provided by the RegCM3 simulations (See Section 2.1) for the entire study period (195–2100). The calculation of the horizontal wind stresses, used in the momentum equations, is based on the wind velocity data at 10 m above mean sea level:

$$\tau_{sx} = \rho_A C_s |\mathbf{W}| W_x \& \tau_{sy} = \rho_A C_s |\mathbf{W}| W_y \tag{1}$$

where ρ_A is the air density, $\mathbf{W} = (Wx, Wy)$ is the wind velocity horizontal vector, with its norm given by $|\mathbf{W}| = \sqrt{W_x^2 + W_y^2}$, and C_s is a coefficient quantifying friction on the sea–air interface. The sea surface friction coefficient used in the present model is calculated following the approach of Smith and Banke (1975):

$$C_s = \frac{(0.63 + 0.066|\mathbf{W}|)}{10^3} \tag{2}$$

Bottom friction is taken into account by our model, with the use of the classical expression for the bed stress, $\boldsymbol{\tau}_b = \rho_w C_D |\boldsymbol{u}_b| \boldsymbol{u}_b$, where ρ_w is the water density and $\boldsymbol{u}_b$ is the velocity vector on the bed. The related bottom friction coefficient, C_D, is specified to match the law of the wall in the bottom logarithmic layer (Wang, 2002):

$$C_D = \max\left\{\left[\frac{1}{k}\ln\left(\frac{H}{z_o} + 1\right)\right]^{-2}, 0.0025\right\} \tag{3}$$

where $\kappa \approx 0.41$ is the von Kármán constant, H is the total water depth and z_o is the sea-bottom roughness, here set equal to 0.001. The computation of the horizontal eddy viscosity distribution is based on a Smagorinsky-type diffusion scheme.

The atmospheric pressure contribution is included in the momentum equations in terms of a pressure gradient $dp_a/dl \times 1/\rho$, where p_a is the atmospheric pressure, ρ is the seawater density and l is the longitudinal (x) or latitudinal (y) spatial coordinate of the Cartesian model grid. The model domain is presented in Fig. 1a (the areas of the Black Sea and

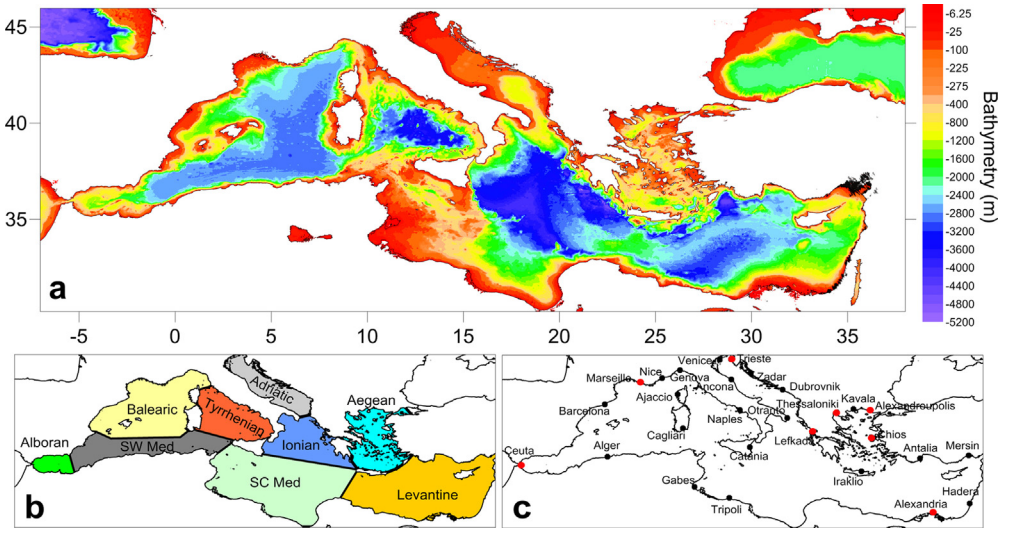

Fig. 1. Maps of (a) the Mediterranean Sea bathymetry (m) and of the MeCSM model domain (Atlantic and Black sea excluded), (b) the regional seas (SW: SouthWestern, SC: South-Central) and (c) 8 tide-gauge stations (red dots) and 20 additional locations (black dots) used in the study. (For interpretation of the references to color in this figure legend, the reader is referred to the web version of this article.)

Atlantic Ocean are excluded from the calculations). The General Bathymetric Chart of the Oceans (GEBCO; http://www.gebco.net/) was used to build the model bathymetry with bilinear interpolation into the model's computational grid.

2.3. SLH observations

In situ sea level data were collected from two sources. Data from the Global Sea Level Observing System (GLOSS; http://www.gloss-sealevel.org/) were used for the broader Mediterranean region (4 stations) and data from the Hellenic Navy Hydrographic Service (HNHS; http://www.hnhs.gr/portal/page/portal/HNHS) were used for the topographically diverse Greek seas (4 stations). The GLOSS data were obtained by the University of Hawaii Sea Level Center (UHSLC; http://uhslc.soest.hawaii.edu/home). Daily-averaged values, based on high-quality (10 min samples) measurements, were collected from the 4 GLOSS stations, namely Marseille, Ceuta, Trieste and Alexandria (Fig. 1c), in order to evaluate the validity of the MeCSM climatic simulation. The recording periods correspond to 1998–2007 and 1951–2008 for Marseille and Ceuta, respectively, while the available data for Alexandria and Trieste cover only a small time-span from 2009 to 2012. In addition, available data from three stations in the Aegean Sea (Thessaloniki, Alexandroupolis, and Chios) and one in the Ionian Sea (Lefkada), collected from the HNHS network, cover the period of 2002–2012. The collected data relate to different periods and regions of the Mediterranean Sea and therefore can be characterized as representative of the sea level variability of the entire region. The collected data refer to a large part of the control run period (*e.g.* Ceuta, Marseille) and, in some cases (*e.g.* Alexandria, Trieste and Greek stations), also cover a few years from the beginning of the climatic scenario simulation. The data from stations over the control period (up to 2000) are more adequate for the model validation, since the respective RegCM3 forcing refers to actual historical emission conditions. However, the data from the first decade of 21st century (up to 2012) are also considered acceptable for model validation, since all the near-future (first decade of 21st century) emission projections follow the trends of the historical measured emissions (low CO_2 variability between different IPCC scenarios during this early-stage period; IPCC, 2001).

In the cases of both GLOSS and HNHS stations, the daily-averaged SLH values, used in the study, were derived from the measured data after subtraction of the mean sea level, which was determined using a moving average technique. Thus, all observed SLH time-series were processed using a heuristic technique, which consisted of a high-pass filter operator with a cut-off frequency of 1/30 days, in order to exclude long term oscillations of the sea level (Conte and Lionello, 2013). The latter can be primarily induced by the steric effects, due to the large-scale, low-frequency, thermohaline fluctuations and/or total mass variations of the enclosed basin under investigation (Carillo et al., 2012). Additionally to the density-based steric effects, mass changes of the whole Mediterranean Sea take place due the flow exchanges with the neighboring Atlantic Ocean (Criado-Aldeanueva et al., 2008). All the aforementioned types of effects are not simulated by MeCSM, which considers the Mediterranean region as an enclosed aquatic body and, thus, such influences needed to be excluded from the observations, as well. In general, an attempt was made to remove all low- frequency oscillatory components from the available gauge time-series. Conclusively, in all following comparisons of model output against available tide-gauge data, only daily-averaged values are used for both simulated and recorded SLH data.

Moreover, the MeCSM model does not include modeling of the astronomical tides. However, given that in most of the considered stations (in the Mediterranean) the tidal cycle is of the semi-diurnal type, the use of daily-averaged SLH values practically excludes the need for tidal simulation. The records present two high and two low tidal values of approximately equal range every lunar day, thus a daily-averaged value of the recorded time-series implicitly removes almost all of the tidal effects in the signal; although the semidiurnal component has a period of 12.4 h instead of 12 h, the daily-averaged value is efficient to calculate the statistical variables (*e.g.* occurrence frequencies of local peaks, percentiles) used to evaluate the long term climatic simulations. Discrepancies due to explicit daily averaging are very small compared to the increase of SLH due to storm surges. Astronomical tides are of generally small amplitude ($<$0.5 m) in the Mediterranean Sea, compared to the extreme positive and negative free surface elevation due to storm surges. This is not necessarily true for the N. Adriatic where the tidal signal can add up to 30 cm on the 50-year return period SLH, according to Marcos et al. (2009); tidal gauge data are used for comparison only in Trieste for the N. Adriatic region.

2.4. Statistical significance of trends

In order to evaluate the statistical significance of the trends for simulated storm surge features under climatic scenario future conditions, the Mann–Kendall (MK) test (Mann, 1945; Kendall, 1975) is used. The purpose of the MK test is to statistically assess if there is a monotonic upward or downward trend of the variable of interest over time and it is widely used for the analysis of trend in climatologic time-series (Mavromatis and Stathis, 2011). The MK test can be used in place of a parametric linear regression analysis, which can be used to test if the slope of the estimated linear regression line is different from zero. According to this test, the null hypothesis assumes that there is no trend (the data is independent and randomly ordered) and this is tested against the alternative hypothesis, which assumes that there is a trend (Onoz and Bayazit, 2003). If the p- value, computed by the MK test, is less than the considered significance level (*e.g.* 5%), the null hypothesis that there is no trend, is rejected. We chose the 95% confidence level, which indicates 5% tolerance ($a = 0.05$), in order examine the statistical significance of a trend. Rejecting the null hypothesis (p-values $< a = 0.05$) indicates that there is a trend in the time-series, while accepting the null hypothesis (p-values $> a = 0.05$) indicates that no significant trend was detected. On rejecting

the null hypothesis (no trend), the result assumed to be statistically significant (the risk in rejecting the null hypothesis is lower than 5%).

3. Model evaluation

The SLH time-series from the MeCSM simulations are compared with *in situ* observations from eight tide-gauge stations (Section 3.1) in order to validate the storm surge model results. Daily SLH measurements are compared with corresponding model results during specific periods. The simulated time-series cover the exact same periods with the respective available observations and refer to the closest model grid point for each one of the 8 gauge stations. An additional evaluation using a realistic simulation (hindcast run) is presented in Appendix A, in order to validate the barotropic climatic model, used in the current study.

3.1. Comparison of local maxima

We calculated the local SLH peaks for four stations (Ceuta, Marseille, Trieste and Alexandria) covering the Mediterranean Sea from West to East, in order to assess the performance of the model in coastal sub-regions with different topographic characteristics. The local peak computation compares all daily-averaged SLH with its neighboring values; if a daily value is larger than both of its "neighbors", then this SLH value is defined as a local peak. The local peak frequency of occurrence, presented in Table 2, is derived from the number of days that local maxima appeared in the SLH time-series, divided by the total number of days of each period of comparison. For each station, all local peaks that exceed 20 and 30 cm were computed, in order to evaluate the model during periods of high positive surges. The comparison of local peaks' frequency, between model and *in situ* data, shows that the agreement is satisfactory in all stations (Table 2).

The 10-year period comparison at Marseille shows local peak frequencies around 20% for both model (22.3%) and *in situ* (18%) time-series (Table 2). Local peaks that exceed the elevation of 20 cm also present similar occurrence frequencies between model output and observations (1–2%). We calculated contiguous but slightly smaller frequencies of occurrence for a station in the western Mediterranean (Ceuta; Table 2), while the extreme local peaks (>20 cm) are almost negligible, indicating the predominance of low SLHs in the western Mediterranean. In the N. Adriatic Sea, we derived higher values (Trieste; Table 2) for both model (23.8%) and measurements (19.6%), while the frequencies of local peaks over 20 cm are in very good agreement (∼2.6%) for both time-series. Significant local peak frequencies for SLH over 20 cm were observed only in Trieste. This observation is in agreement with previous studies that found the highest SLH values of the Mediterranean over the northern Adriatic area (*e.g.* Marcos et al., 2009). Based on observations and simulations, Conte and Lionello (2013) showed that the largest SLHs of the entire Mediterranean coastal region occur in Trieste, with generally smaller surges outside the Adriatic. The northern Adriatic Sea reveals the highest sea level values for both model and measurements, mainly due to wind forcing mechanisms (discussed further in Section 4.1). The calculated occurrence frequency of SLH local peaks is very low for the southeastern station of Alexandria (<4%; Table 2), while the frequency of local peaks exceeding 20 cm, derived from both MeCSM and *in situ* time-series, is zero.

Our results generally tend to underestimate local peaks over 30 cm, especially in areas like Trieste. On the other hand, the results are more satisfactory for the case of lower peaks (>20 cm); MeCSM predicts values closer to the measured data, apart from Ceuta, where the error is higher due to the proximity to the Gibraltar strait (discussed further in Section 3.2). However, the objective of the work is to investigate future trends, frequencies and seasonal changes of surge events over the Mediterranean, and thus this underestimation does not significantly change the main findings of the work, since it exists in both the control and the scenario runs. The spatial distribution of surge maxima over the basin is adequately predicted by the model, as shown in Table 2 and in following results, improving the confidence of the climatic storm surge projections. Overall, the estimations of the present work seem to have an inherent under-prediction of peak SLHs that affects mainly the values of surge maxima and not the general trends, the spatial distribution and the seasonality of extremes.

Table 2
Comparison of occurrence frequencies (%) of SLH local peaks, from daily-averaged *in situ* and respective MeCSM data, for all recorded maxima and for maxima exceeding the thresholds of 20 and 30 cm; the stations include Marseille (1998–2007), Ceuta (1951–2008), Trieste (2009–2012) and Alexandria (2010–2012).

Station	Period	All (%)		>20 cm (%)		>30 cm (%)	
		MeCSM	*In situ*	MeCSM	*In situ*	MeCSM	*In situ*
Marseille	1998–2007	22.3	18	1.1	1.7	0	0.5
Ceuta	1951–2008	20.6	17	0	0.6	0	0.1
Trieste	2009–2012	22.8	19.6	2.6	2.7	0.3	1.6
Alexandria	2010–2012	3.3	2.1	0	0.1	0	0

3.2. Storm Surge Index

The statistically significant values of the largest annual sea level anomalies can be investigated using the Storm Surge Index (*SSI*). *SSI* is defined as the average of the three (3) highest independent storm surge maxima per year (Conte and Lionello, 2013). As suggested by Conte and Lionello (2013), only events separated by at least 120 h (estimation of the maximum duration of a storm) are considered as independent storm events and are thus used to calculate the *SSI* values for each station. The *SSI* for both simulated and observed time-series was calculated for each of the eight stations, along with the corresponding Percent Error (*E*):

$$E(\%) = \frac{\overline{SSI}_{mod} - \overline{SSI}_{obs}}{\frac{\overline{SSI}_{mod} + \overline{SSI}_{obs}}{2}} \times 100 \tag{4}$$

where $\overline{SSI}_{mod}$ and $\overline{SSI}_{obs}$ are the mean *SSIs* over the periods of comparison as derived from modeled and observed data, respectively. *E* is positive when the model overestimates the amplitude of the sea level against observed data. In order to provide more information about the significance of the error, the Error Index (*EI*) is also calculated according to the following relation (Conte and Lionello, 2013):

$$EI = \frac{\overline{SSI}_{mod} - \overline{SSI}_{obs}}{\sqrt{\frac{\sigma^2_{SSI_{mod}} + \sigma^2_{SSI_{obs}}}{2}}} \tag{5}$$

where σ is the standard deviation of the interannual variability of *SSIs* corresponding to either the simulated (mod) or observed (obs) time-series for each station.

High *SSI* values occur over the northern Adriatic coastal region (Trieste), where both modeled and observed *SSIs* are around 30 cm (Fig. 2a), with the lowest Percent Error (~6.8%; Fig. 2b), supporting the good performance of the model. Small overestimation of the simulated *SSIs* in comparison with the *in situ* data (*EI* = 0.29; Fig. 2b) is detected, in agreement with

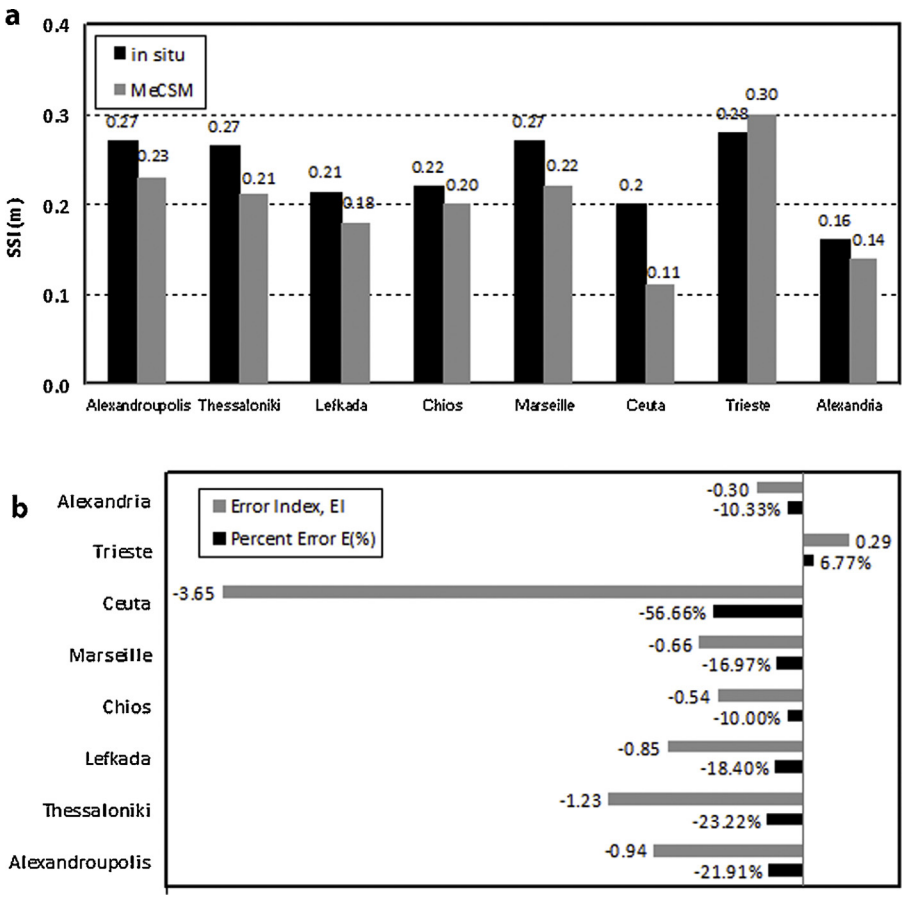

Fig. 2. Comparison between MECSM and *in situ* time-series, for the 2002–2012 period, concerning (a) Storm Surge Index (*SSI*) values, (b) Percent Error (%), and Error Index values at Chios (Central Aegean), Lefkada (Ionian Sea), Thessaloniki and Alexandroupolis (North Aegean), Alexandria (South Levantine), Trieste (North Adriatic), Ceuta (West Alboran), and Marseille (North Balearic).

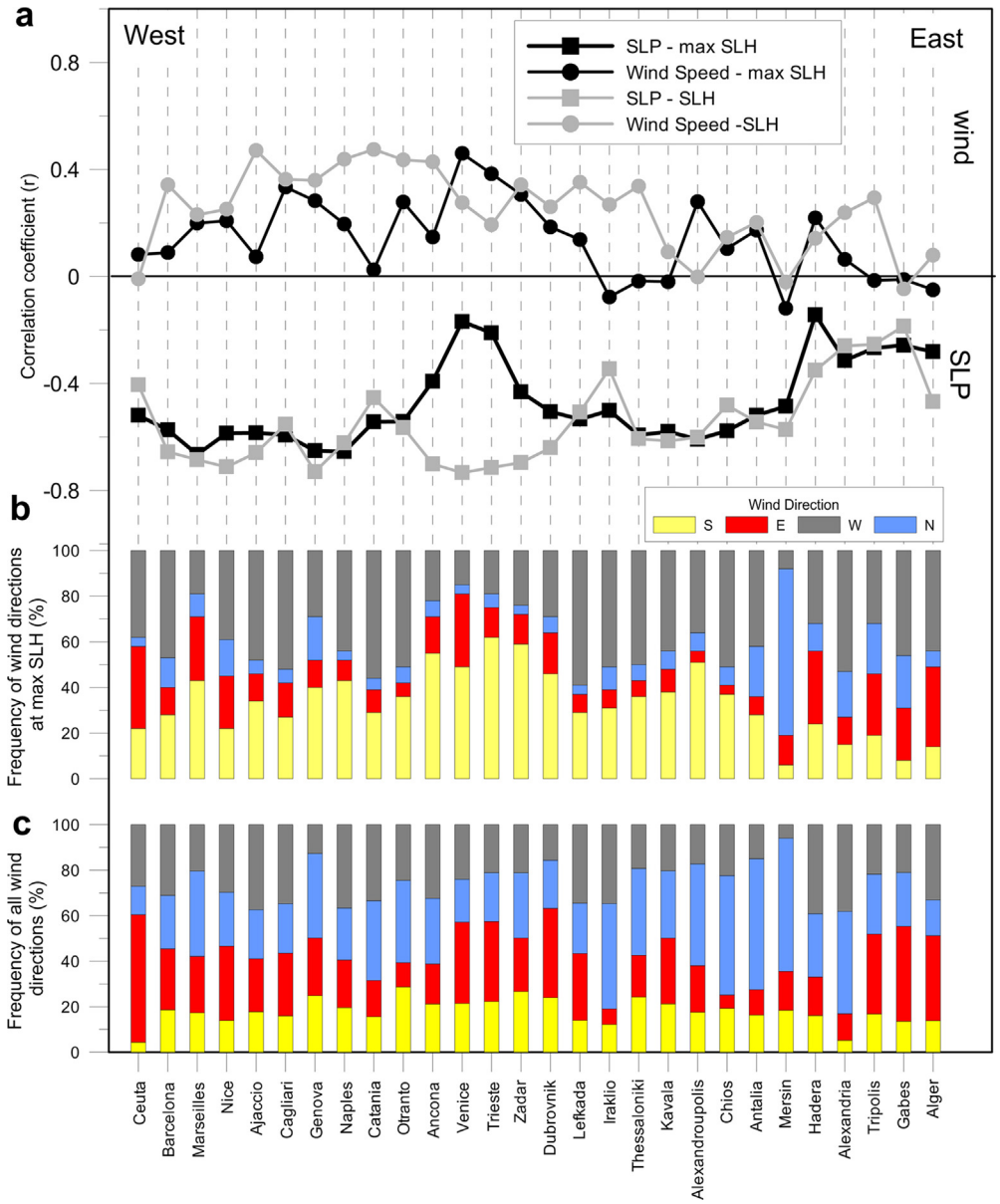

Fig. 3. (a) Distribution of Pearson product- moment correlation coefficients (r) between the annual maximum SLH and the respective SLP (black squares) and wind speed (black circles) values for 28 Mediterranean locations, derived for the entire future period (2001–100). The corresponding correlations for the averaged values (entire time-series) of SLH, SLP and wind speed are indicated with gray color. Occurrence frequency of the cardinal wind directions (b) for the entire future period and (c) during annual maximum SLHs for the 28 study locations, as derived from the RegCM3 climatic scenario run.

Conte and Lionello (2013), who showed small positive *EIs* only at stations of the N. Adriatic ($SSI_{mod} > SSI_{obs}$; their Fig. 3a). Even though the model underestimates the *SSI* at all other stations (negative *EI* values), the error is generally small and SSI_{mod} and SSI_{obs} values are very close. The Ceuta station is an exception with higher errors ($|E| > 50\%$; $EI = -3.65$), probably due to discrepancies of the old time-series of measured SLH (starting in 1951). Moreover, the error over this region that neighbors the Atlantic may be related to the assumption of a closed western boundary by the barotropic simulation, which does not take into account the mass contribution from the Atlantic (Calafat et al., 2012). However, both control run results and observations show low *SSI* values (<20 cm), supporting the low presence of SLH extremes in the area due to meteorological conditions. Although the model underestimates the magnitude of surges, it still performs well in terms of predicting the frequency of local peaks over this western-most region (Table 2). Conte and Lionello (2013) also showed results of climate storm surge simulations with significantly high E (>40%) and similar underestimations of the simulated SLHs over coastal

Table 3
Comparison of occurrence probabilities of coherent (P_{coh}) and intense (P_{int}) events for Greek stations, from *in situ* and respective MeCSM data.

Station	P_{coh} (%)		P_{int} (%)	
	MeCSM	*In situ*	MeCSM	*In situ*
Alexandroupolis	14.0	15.0	3.5	3.2
Thessaloniki	15.0	15.0	3.3	3.6
Lefkada	15.4	14.6	3.7	4.0
Chios	14.3	14.0	3.6	3.5

regions of the western Mediterranean. Lower errors (in absolute values) are derived at the stations of Marseille ($E = -16.7\%$; $EI = -0.66$) and Alexandria ($E = -10.33\%$; $EI = -0.30$), where the modeled *SSIs* are around 22 cm and 14 cm, respectively.

The 11-year recordings of daily-averaged SLHs from four stations along the Greek coastal zone were also used to evaluate the model's performance over this topographically complicated region. The lowest *SSI* values in the Greek coastal zone were calculated in the Ionian Sea (Lefkada) (Fig. 2a), as derived from both simulated and observed time-series. The highest values (27 cm) were observed at the northern Aegean stations. Although the model underestimates the respective annual extremes, it produces the highest values (~22 cm) among the Greek stations over the same region, in agreement with observations. The largest (absolute) *EI* for the Greek stations was calculated in Thessaloniki ($EI = -1.23$; Fig. 2b). Conte and Lionello (2013), based on a 7-member climate model ensemble, presented similarly high errors at several Mediterranean stations (their Fig. 3c). Other Greek stations display smaller $|E|$ (<20%) and $|EI|$ (<1), indicating that the simulation errors, as derived from the comparison with the observed data, are not significant.

Overall, the linear regression coefficient, between all model and observed mean *SSI* values (calculated for all stations presented in Fig. 3a), equals 0.85. In addition, the Pearson correlation coefficient as derived between the 8 stations is 0.81; both indexes are close to 1. All above comparisons of measured and simulated *SSIs* shows that, apart from the western-most area near the Gibraltar strait, the model performs adequately. The impact of the error in the vicinity of the strait is highly localized and does not affect the other areas of the basin; the comparison in Marseille, an area of the western Mediterranean coastline, is good, with rather low absolute error values (Fig. 2b). Furthermore, the low absolute *EI* values indicate that the impact of the simulation errors on the estimation of storm surge extremes' evolution due to future climatic conditions is also expected to be small, adding confidence to our investigation.

3.3. Comparison of coherent extreme events

In a study about the intermittency of coastal sediment transport and surf zone turbulence, Jaffe and Sallenger (1992) heuristically defined the events that exceed certain critical values, as 'coherent' and 'intense' extreme events. A similar approach is used in the present study; a coherent event is defined as having values of $SLH_{coh} \geq (m + \sigma)$, where m is the mean of the *SLH* time-series over the entire study period (11 years in the case of the Greek stations), and σ is the corresponding standard deviation (Jaffe and Sallenger, 1992; Cox and Kobayashi, 2000). The probability of occurrence of coherent events (P_{coh}) for all Greek stations is presented in Table 3, as derived from both simulated and observed time-series. In addition, the occurrence probability of intense events (P_{int}), which are defined as $SLH_{int} \geq (m + 2\sigma)$, is also presented in Table 3, describing the frequency of significantly extreme and rare events. Simulated values are correlated well with the measured ones in all stations, with low frequencies of intense events over the N. Aegean (Thessaloniki and Alexandroupolis), and higher values over the Ionian Sea (Lefkada). Even though Lefkada showed the lowest *SSI* values (Fig. 2a) in the Greek seas, the P_{int} occurrence probability is the highest of all Greek stations. It follows that, this area shows frequent, but low in magnitude, SLH extremes. Both model and *in situ* values support this finding, indicating the good performance of the model between different areas. More discussion on the spatial variability of SLH extremes is included in Section 4.1.

Table 4
High order (80th, 90th, 95th) percentiles (Per) of SLH (cm) at Chios (Central Aegean), Lefkada (Ionian Sea), Thessaloniki and Alexandroupolis (North Aegean), Alexandria (South Levantine), Trieste (North Adriatic), Ceuta (West Alboran), and Marseille (North Balearic) Stations, derived from both MeCSM (Per_{mod}) and *in situ* (Per_{obs}) data.

Per station	80th		90th		95th	
	Per_{mod}	Per_{obs}	Per_{mod}	Per_{obs}	Per_{mod}	Per_{obs}
Alexadroupolis	7.5	7.3	11.5	12.9	14.0	18.6
Thessaloniki	6.9	6.7	10.7	12.0	14.0	16.0
Lefkada	5.7	5.9	9.2	10.4	12.3	14.0
Chios	7.1	5.8	10.4	10.3	13.4	14.5
Marseille	6.8	7.2	12.3	13.4	16.3	18.7
Ceuta	2.2	5.5	4.1	9.4	5.9	13.1
Trieste	8.0	9.8	13.2	17.9	18.0	24.9
Alexandria	7.1	10.7	9.1	13.7	11.5	15.9

3.4. Comparison of high-order percentiles

The performance of the model was also evaluated by the use of high-order percentiles (80th, 90th, and 95th), presented in Table 4. The highest values were derived for the N. Adriatic (Trieste) from both simulated and observed data, in agreement with the occurrence frequencies of high local peaks (Table 2) and the respective *SSIs* (Fig. 2a). The lower *SSIs* for the Ionian Sea (Lefkada; Fig. 2a) are also confirmed by the percentile levels; all percentiles, derived from the Lefkada data, are smaller than the respective values from the Aegean stations (Thessaloniki, Chios, and Alexandroupolis). For example, the 80th percentile at Lefkada is 5.7 cm from model output and 5.9 cm from measurements, while the respective percentiles (*Per*) from the Aegean stations (*e.g.* Thessaloniki and Alexandroupolis) may reach a level of 7.4 cm (Table 4). Similarly, the higher order 95th percentile is 12.3 and 14.0 cm, derived by simulations and measurements respectively. This indicates that the extreme events of the Ionian region are weaker in comparison with those at the N. Adriatic Sea (*e.g.* Trieste: Per_{mod} = 18.0 cm and Per_{obs} = 24.9 cm) and the Aegean Sea (*e.g.* Thessaloniki: Per_{mod} = 14.0 cm and Per_{obs} = 16.0 cm). Although Ceuta shows poor agreement between simulated and observed data, both time-series revealed the lowest percentiles among all stations. At the French coast, the relevant comparisons in Marseille show very good agreement, namely for the 80th (Per_{mod} = 6.8 cm and Per_{obs} = 7.2 cm), 90th (Per_{mod} = 12.3 cm and Per_{obs} = 13.4 cm), and 95th (Per_{mod} = 16.3 cm and Per_{obs} = 18.7 cm) percentiles. Generally, the percentiles computation of the 8 stations showed similar behavior for both model and measurements indicating that the simulation of the *Past Period* follows the regional surge characteristics of the Mediterranean Sea, as derived from the available gauges.

4. Long-term climatic simulations

The contribution of wind and SLP on the SLH variability differs from region to region, depending on topographic and morphological features. This contribution on the SLH evolution and its seasonal variability along the Mediterranean coastline (28 locations, involving 8 stations, presented in Fig. 1c) and over the Mediterranean sub-basins (9 regional seas, presented in Fig. 1b) are investigated using results from the 1951–2100 climate simulation.

4.1. Atmospheric contribution on evolution of extreme events

The interannual evolution of the annual maximum SLH (SLH_{max}) for all study stations, covering the greater part of the Mediterranean coastal zone, was derived from the long-term climatic simulation and is discussed below (Section 4.1.1). In order to further investigate the contribution of the two atmospheric forcing factors (SLP and wind) on the SLH variability over different regions of the Mediterranean Sea, we performed two additional idealized numerical experiments, by separating each forcing factor and examining its individual effect on the SLH trends (Section 4.1.2).

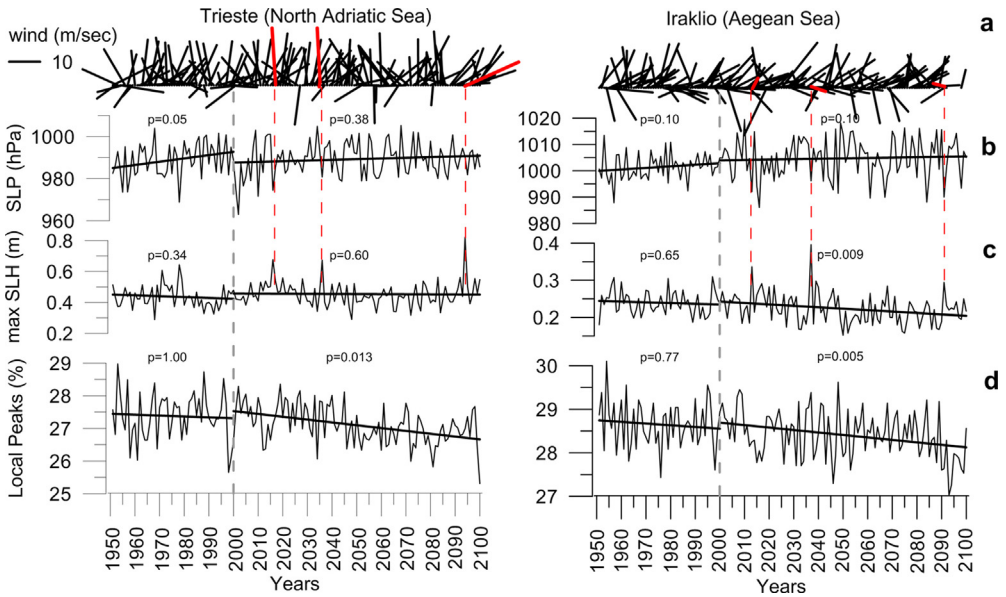

Fig. 4. Climatic evolution of (a) wind (m/sec), (b) SLP (hPa) from the RegCM3 simulation, (c) annual maximum SLH (m), and (d) occurrence frequency (%) of SLH local peaks from the MeCSM simulation in Trieste (North Adriatic; left panel) and Iraklio (Aegean Sea; right panel). The linear trends for the *Past* and *Future Periods* are indicated with a thick solid black line and the three highest annual SLH maxima of each station are indicated with red color. The *p*-value (*p*) for each time-series is presented at all panels. (For interpretation of the references to color in the text, the reader is referred to the web version of this article.)

4.1.1. Interannual SLH evolution, based on climatic simulation

The interannual evolution of the annual maximum SLH for all study locations, covering the greater part of the Mediterranean coastal zone, was derived from the future long-term 100-year (2001–2100) simulation, under climatic scenario A1B (*Future Period*). Fig. 3a presents the correlation coefficients of SLH with the corresponding SLP (squares) and wind speed (circles) values; these values are calculated, both from the entire time series (SLP- *SLH*, gray squares; *Wind Speed-SLH*, gray circles) and only during maximum storm surge annual events (*SLP-max SLH*, black squares; *Wind Speed-max SLH*, black circles). Fig. 3b and c presents the occurrence frequencies of the four cardinal wind directions during maximum events and nominal values (entire period), respectively. As expected, the SLHs are generally inversely correlated to the SLP values and positively correlated to the wind velocity (Fig. 3a). The low pressure systems may affect the sea level in coastal regions directly underneath the eye of the cyclone (inverse barometer), showing correlation coefficients lower than −0.4 (Fig. 3a) for the majority of the study regions. The accumulation of waters near the shore due to direct wind effect is of lower influence on the SLH magnitude in most areas (<0.4; Fig. 3a).

The French Mediterranean coast (*e.g.* Marseille), the central western Italian coast (*e.g.* Naples) and the N. Aegean coastal region (*e.g.* Thessaloniki) show strong correlation between extreme SLHs and pressure, with coefficients around −0.6. The control of SLP over the peak SLHs is more pronounced in the western part of the northern coasts (Ceuta to Catania; black squares in Fig. 3a) with a significantly lower contribution of winds (black circles in Fig 4a). The decrease of wind correlation coefficients toward the East, along the N. Aegean coastline (Thessaloniki to Alexandroupolis; gray circles in Fig. 3a), indicates the low effect of wind on the appearance on SLH variability, which is related to the predominance of northerly winds and the decrease of southerly winds frequency toward the East (Fig. 3c); the occurrence frequency of northerly winds in Thessaloniki, Kavala and Alexandroupolis is significantly high, exceeding 35%, 30% and 40%, while the frequency of southerly winds ranges around 21%, 19% and 17%, respectively. These results agree with the findings of De Vries et al. (1995), who showed that inverted barometer effect is the main controlling factor of storm surges along the N. Aegean coastline. At the same time, an increasing impact of winds from west to east is observed along the N. Aegean coasts (Kavala to Alexandroupolis) during extreme events (black squares in Fig. 3a). This feature is most likely linked to the topography of the area; Kavala is located downwind from a large island (Thasos), while Alexandroupolis is exposed to more open seas (Fig. 1c) and to the impact of southerly winds during surge events; the higher *Wind-max SLH* correlation coefficient in Alexandroupolis (Fig. 3a) is related to the high frequency of southerly winds during the respective maximum SLH events (>40% frequency of southerly winds at max SLH; Fig. 3b). However, low pressure seems to cause the major impact on extreme storm events in all N. Aegean locations, showing significantly high *SLP-max SLH* correlations for the entire *Future Period* (>0.60). Over the southern Aegean (Iraklio), although the highest frequency of all wind directions is for northerly winds (>40%, Fig. 3c), the prevailing winds during extreme storm surge events are from the West (∼50%; Fig. 3b); the northerly winds' frequency, favorable for the accumulation of waters along the coast, is very low (<10%; Fig. 3b). Therefore, although the *Wind Speed-SLH* correlation is relatively high, the *Wind Speed-max SLH* correlation is almost zero. In addition, maximum SLH and pressure are highly correlated (*SLP-max SLH* ∼0.5; Fig. 3a), indicating the strong impact of SLP, especially during extreme storm surge events over this northward-oriented coast.

Contrastingly, the weakest *SLP-max SLH* correlation is detected along the N. Adriatic coasts; Venice and Trieste show coefficients around −0.2. The inverse correlation is gradually increasing southwards along the eastern Adriatic coast and reaches the value of −0.6 over the central Ionian Sea (*e.g.* Lefkada). The time-series of annual maximum SLHs in Venice is well correlated with the respective future wind speed values (>0.4). Almost all of the N. Adriatic locations reveal high occurrence frequency of easterly and southerly winds (>60% in summation, Fig. 3b) during strong surges, which are most frequent during colder periods (Pandžić and Likso, 2005). The effect of Sirocco winds in combination with seiches may increase the risk of flooding over the N. Adriatic coastal areas (Vilibic, 2000 Marcos et al., 2009). Although the correlation between pressure and sea level height during extreme events (*SLP-max SLH*) is low over the N. Adriatic coasts, in agreement with previous findings (*e.g.* Orlić et al., 1994; Pirazzoli and Tomasin, 2002; Lionello et al., 2006; Krestenitis et al., 2011), calculating the correlation coefficients from the entire time-series (using all daily values, *SLP–SLH*) reveals a strong relation between the two parameters ($r < -0.70$; gray square points in Fig. 3a). It seems that strong southeasterly Sirocco winds may accumulate surface water masses over the enclosed N. Adriatic coastal region, producing sea surges (Pirazzoli and Tomasin, 2002), but during periods with higher pressures and weaker winds (high pressure systems), the sea level mainly follows the variability of pressure.

The Adriatic and Aegean Seas are two major Mediterranean basins with special morphological features that have been affected by significant storm surges in the past (Krestenitis et al., 2011). To elaborate further on the storm surge characteristics and the related driving mechanisms for the entire study period (*Past* and *Future Periods*), we investigate the storm surge extremes' evolution and trends using one coastal station from each area (Trieste and Iraklio). The *p*-value (see Section 2.4) is computed for both *Past* and *Future* periods, presented in Fig. 4 for Trieste and Iraklio.

The MeCSM simulation, under A1B scenario, reproduced maximum SLHs that may reach 80 cm in Trieste (Fig. 4c). Focusing on the peak SLHs in Trieste in the *Future Period*, we detect 3 strong events (SLH > 60 cm), corresponding to 2016, 2036 and 2094. We refer to specific years, not as a precise forecast of future events (*i.e.* one of the storms is expected to happen in 2016), but as indicators that aid the visual detection of these events in the plot (Fig. 4) and the related investigation of future extreme surges due to atmospheric conditions. The prevailing strong southerly winds (>20 m/s) over the Adriatic Sea during these storms are responsible for high sea surface elevations (red vectors in Fig. 4a). Although the SLP trend is not statistically significant ($p = 0.38 > a = 5\%$), it shows slightly higher values than the previous period. At the same time, the

interannual evolution of maximum SLH is essentially stable during the *Future Period* (very high p-value ~0.60). Moreover, the *Past Period* is characterized by a very weak decreasing trend of SLH maxima. This is the case in spite of the fact that there is a strongly increasing SLP trend (slope = 0.16 ± 0.08 hPa/year and $p = 0.05$) during this period, that, however, seems to not affect the SLH maxima. The latter is in agreement with the low correlation between the annual maximum SLH and the corresponding SLP values (Fig. 3a). The MeCSM simulation also shows a slightly decreasing trend for the frequency of local peaks (slope = −0.002 ± 0.005%/year and $p = 1 > a = 0.05$; Fig. 4d) during the *Past Period,* in agreement with the observations of Raicich et al. (2003), who showed that in the 1940–2001 period, the frequency of strong positive surges exhibited a likely small negative trend, whereas trends of lower surges were stable. Contrastingly, the annual frequency of local peaks decreases more rapidly (slope = −0.022 ± 0.01%/year and $p = 0.013$) during the entire 21st century (*Future Period*). This indicates that even though a few greater extremes may occur in the future and the SLH maxima trend is almost stable, the total number of local peaks may decrease, most likely due to the generally high values of SLP (Fig. 4b). This increase of SLP is probably related to the increasing anticyclonic atmospheric circulation over the Mediterranean, which may cause a northward shift of the mid-latitude storm tracks (Giorgi and Lionello, 2008). The general trend of all SLH values in Trieste is affected mainly by pressure ($r = -0.72$; gray square in Fig. 3a), while the extreme values are controlled by the strong southerly winds ($r = 0.35$, black circle in Fig. 3a).

The relation between atmospheric conditions and extreme surge events in the Aegean coastal region (Iraklio) is different. The maximum SLHs present a decreasing tendency in the *Past Period* that is inversely correlated with the increasing trend of the SLPs (slope = 0.07 ± 0.06 hPa/year and $p = 0.10$); although the risk to reject the no trend hypothesis, in this case, is higher than the confidence level of 5%, it is still relatively small (10%). Annual maximum SLHs in Iraklio continue to drop in the entire *Future Period* following a statistically significant decreasing trend (slope = −0.4 ± 0.2 mm/year and $p = 0.009$; Fig. 4c), while the respective SLPs show a continuous increase (Fig. 4b). Moreover, the local peak frequency also shows a respective decreasing trend during the entire study period (slope = −0.024 ± 0.01%/year and $p = 0.005$; Fig. 4d). Similar to the N. Aegean locations, the correlation coefficient of maximum SLHs and wind speed values in Iraklio is very small and negative ($r = -0.05$; gray circle in Fig. 3a), indicating the complete irrelevance between the two parameters. The prevailing southwesterly winds, during extreme events in Iraklio (>90%, Figs. 3 b and 4 a), are unfavorable for accumulating waters near the shore. The highest extreme SLHs exceed 0.3 m (*e.g.* 2013, 2037 and 2091) and coincide with very low pressures (~990 hPa; Fig. 4b) and unfavorable weak winds (red vectors in Fig. 4a), indicating the direct effect of low pressure systems on the surge level variability of this coastal area. Analogous findings for other Aegean locations (not shown) suggest that pressure is the main factor controlling extreme storm surge events over the entire region.

4.1.2. Interannual SLH evolution, based on idealized experiments

In order to elaborate further on the driving mechanisms of storm surges in the Mediterranean and to explore the future variability under the considered climatic scenario, we obtained results from simulations that took into account separately

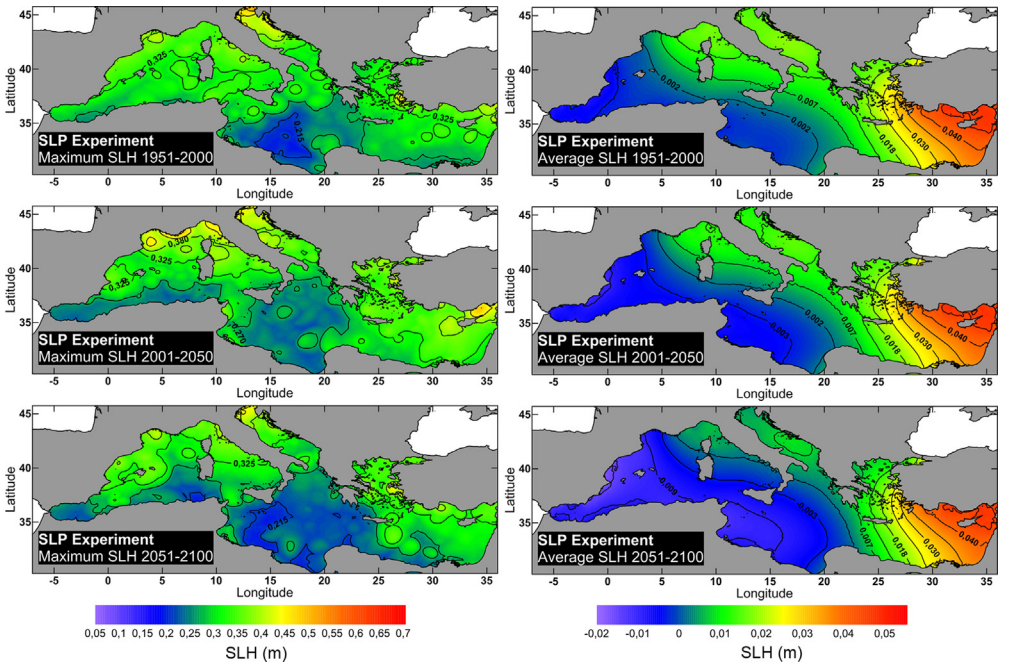

Fig. 5. Horizontal distribution of maximum (left) and average (right) SLH (m) for the 1951–2000, 2001–2050, and 2051–2100 periods, as derived from the *Pressure Experiment* (only SLP forcing).

the effect of pressure (*Pressure Experiment*: without winds) and the effect of winds (*Wind Experiment*: without SLP gradient). The study period is divided in three equal time spans, the *Past Period* (1951–2000), the first (2001–2050) and the second (2051–2100) half of the *Future Period* (A1B scenario). Results from the two distinct simulations were used to calculate the maximum and the average SLHs for each 50-year period, presented in Fig. 5 for the *Pressure Experiment* and Fig. 6 for the *Wind Experiment*. The frequency of occurrence for each cardinal wind direction, averaged over each region and each 50- year period, is presented in Fig. 7. These experiments confirm the previous findings regarding the atmospheric contribution to the SLH evolution in the Adriatic and Aegean Seas; in the present section we focus on the driving mechanisms in other regions and on general trends.

The *Pressure Experiment* shows that SLP appears to be the controlling factor of peak SLHs in the Levantine basin, and especially in its northeastern part, as well as along the northern coasts of the Balearic Sea (left panels; Fig. 5); an interesting feature is a general increase of peak SLHs during 2001–2050, compared to the preceding and following 50- year periods. This indicates that an increase of the pressure-driven storm maxima can be expected under the A1B scenario during the first half of the 21st century. Regarding the effect of the atmospheric pressure on the average SLHs (right panels; Fig. 5), a strongly increasing trend from west to east during all periods is observed.

The *Wind Experiment* (Fig. 6) shows a pronounced impact of winds on the peak SLHs in the Gulf of Gabes. This is most likely due to the predominance of easterly winds (Fig. 3c), which, combined with the presence of an extended continental shelf in the gulf of Gabes (Fig. 1a), produces significant accumulation of waters toward the coastal zone. The strong impact of winds also appears for the average SLHs (right panels; Fig. 6), showing that the sea level variation in the area is clearly controlled by wind action. In general, there is a clear distinction of the wind impact between the western and eastern parts of the Mediterranean regarding wind-driven average SLHs, *i.e.* the eastern coastal regions are more influenced by winds. The highest values of SLH can be traced over the northeastern Levantine Sea, with an interesting peak in the coastal zone of Alexandria, which is probably due to the impact of the most frequent northerly winds (Fig. 3c); however, the contribution of winds to average SLHs is much lower (16–50%) than the corresponding contribution of SLPs. Finally, an overall decrease of the wind contribution to the SLHs into the future can be observed by the model results. A reduction of average SLHs is present in the N. Aegean region (right panels; Fig. 6), following the successive occurrence frequency increase of northerly (43.5%, 44.59%, 46.66%) and decrease of southerly winds (18.23%, 17.38%, 16.22%) along the three 50-year periods (Fig. 7). The future p-values for the northerly and southerly occurrence frequencies in Aegean Sea are 0.033 and 0.05, indicating the statistically significant increasing and decreasing trends (slopes of 0.03 ± 0.015%/year and -0.02 ± 0.008%/year), respectively. Similarly, the northerly and southerly winds present a slight increase (27.26%, 27.64%, 28.25%; slope = 0.01 ± 0.048%/year and $p = 0.07$) and decrease (25.59%, 24.55%, 24.39%; slope = -0.01 ± 0.043%/year and $p = 0.08$) respectively in the Adriatic, leading to the attenuation wind-driven average SLHs. This shows that a possible factor for the expected attenuation of storminess under the A1B scenario is the predicted attenuation of the wind contribution to the storm surge frequencies. Contrastingly, the northerly winds over the south-central Mediterranean gradually become more frequent (34.83%, 35.95%, 37.95%;

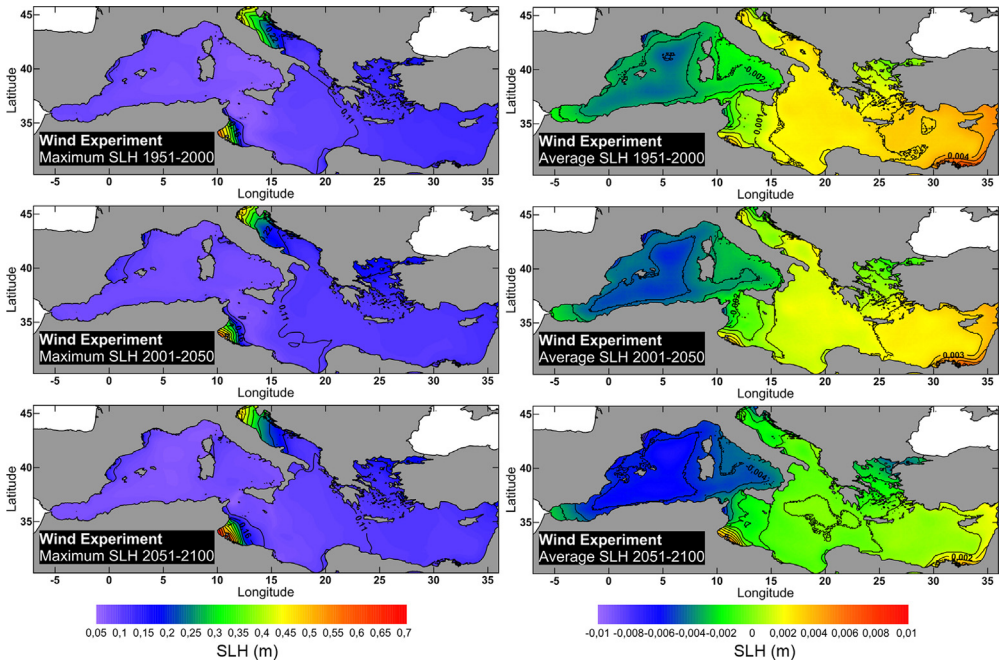

Fig. 6. Horizontal distribution of maximum (left) and average (right) SLH (m) for the 1951–2000, 2001–2050, and 2051–2100 periods, as derived from the *Wind Experiment* (only wind forcing).

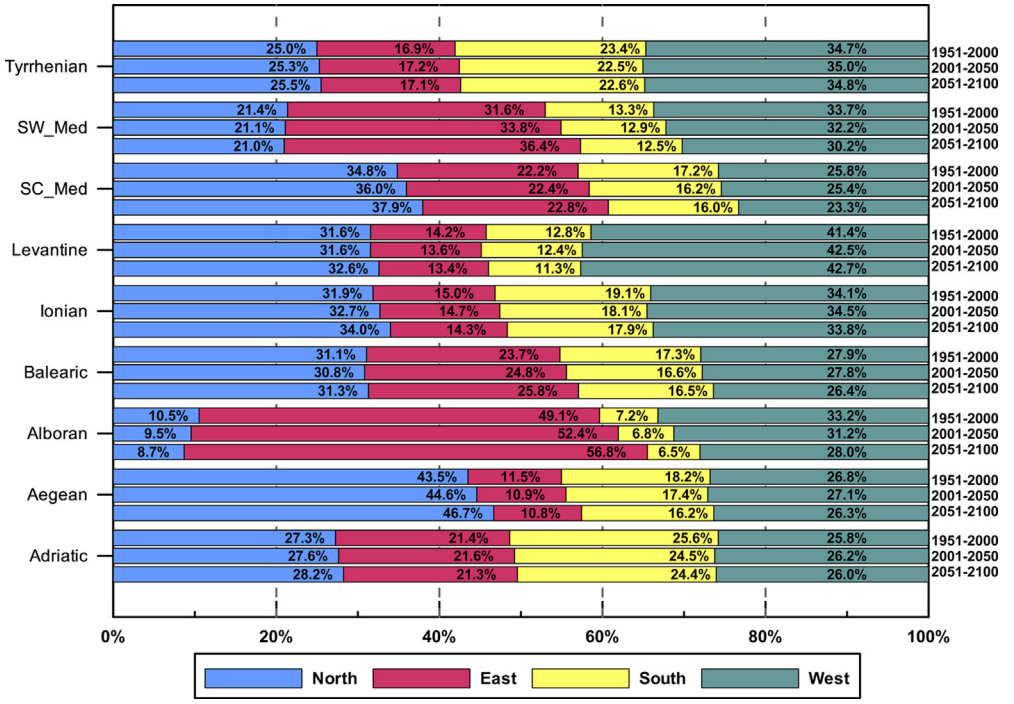

Fig. 7. Occurrence frequency (%) of northerly (blue), easterly (burgundy), southerly (yellow) and westerly (gray) winds, averaged over the nine Mediterranean sub- regions (Fig. 1b) and over the periods of 1951–2000, 2001–2050, 2051–2100. (For interpretation of the references to color in this figure legend, the reader is referred to the web version of this article.)

slope = 0.03 ± 0.01%/year and $p < 0.0001$), increasing the accumulation of waters in the Gulf of Gabes along the three study periods.

4.2. Duration, coverage area and evolution of extreme events

With regard to the investigation of the interannual trends for extreme storm surge events in the regional seas of the Mediterranean region (Fig. 1b), we also examine the temporal evolution of duration, coverage and intensity of surge events. The annual number of 6-h intervals, with a simulated SLH value over 30 cm, can serve as a representative indicator of the severe storm surge event duration per year. In order to assess the spatial extent of these surges, the average number of model grid cells, in which the SLHs exceed 30 cm, is also calculated for each regional sea of the Mediterranean (Fig. 1b). These results are presented in Fig. 8 as red triangles (with reference to the left-hand axis) and blue dots (with reference to the right-hand axis), respectively. The linear trends of these parameters are different for each regional sea and may reveal significant distinctions between the *Past* and *Future Periods.* Almost all regions show a decreasing trend for both temporal (number of 6-hour intervals) and spatial (number of cells) frequencies of severe storms. The statistical significance of these trends is investigated with the computation of the 95% confidence levels (p-values, shown in Fig. 8). The highest and lowest surge durations for all regional seas appear in the first and second half of the *Future Period,* under the A1B climatic scenario, respectively.

The Adriatic presents the highest annual durations of SLHs over 30 cm, confirming the high coastal inundation risk of the area, as discussed in Section 4.1.1. The highest values appear during the first half of the 21st century, while there is a significant decrease during the second half; there is a decreasing future tendency (slope = -0.8 ± 0.3 h/year and $p \sim 5$%), with smaller storm durations and/or fewer storm events near the end of the century. Similarly, the annual storm surge area reduces significantly in the Adriatic Sea during the entire *Past Period* (slope = -0.9 ± 0.24 cells/year and $p < 0.0001$). Although high annual surge coverage was calculated for the 1951–1960 decade (>60,000 km^2), the coverage level dropped below 10,000 km^2 after 1990. Respective but significantly smaller decrease is observed during the *Future Period*, with the coverage area at its minimum during the last decades of the 21st century (slope = -0.03 ± 0.006 cells/year and $p < 0.0001$). High duration values during the same periods were also calculated for the Balearic, Levantine, Tyrrhenian, and Aegean Seas. The lowest values, for both, surge duration and coverage, were computed over the south-central and southwestern Mediterranean (SC Med, SW Med, Ionian and Alboran regions). The majority of these areas show high p-values, indicating the absence of statistically significant trends during both periods under study. However, the coverage area shows higher values during the *Past Period* than the second half of the *Future Period* for these regions, supporting the reduction of storminess over the entire Mediterranean Sea by the end of the 21st century.

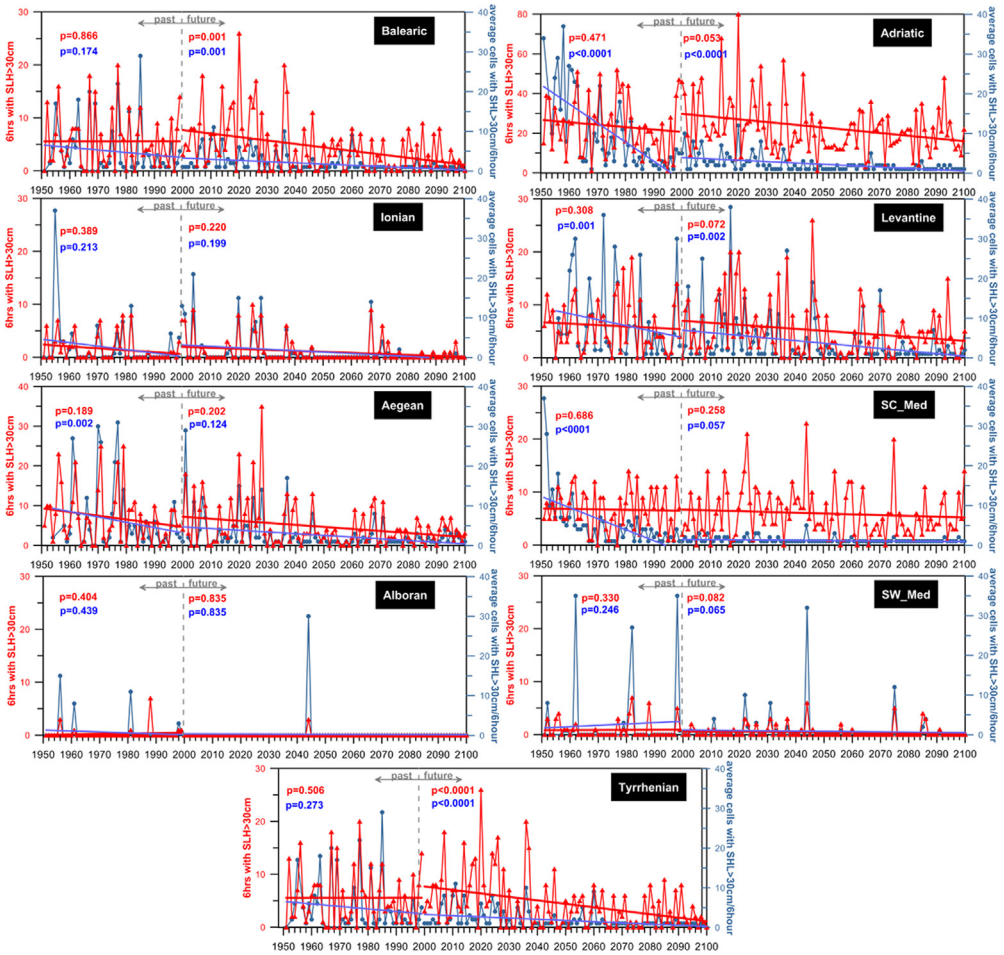

Fig. 8. Annual number of 6-h intervals (red) and the corresponding average number of model cells (blue) with SLH greater than 30 cm for all Mediterranean regional seas (Fig. 1). The linear trends for each parameter and for the *Past* and *Future Periods* are indicated with straight lines. (For interpretation of the references to color in this figure legend, the reader is referred to the web version of this article.)

Fig. 9 presents the annual SLH maxima for each Mediterranean sub-basin, while statistical parameters regarding the presence of linear trends (p-values and slopes) are given in Table 5. Although the SC Med shows significantly low annual surge duration and coverage values, it also presents very high maximum SLHs (>60 cm) due to storm passages, for both *Past* and *Future Periods*. SC Med shows a complete absence of trend for annual maximum values during the entire simulation (1951–2100) (very low confidence levels: $p = 0.97$; Table 5); it is the only region that does not show any decreasing trend during all 50-year periods, presenting an overall stability in SLH variability. Moreover, examining each 50-year period separately, we can note that for 2001–2050 there is a confidently increasing linear trend (slope = $+2.3 \pm 1.0$ mm/year, $p = 0.026$; Table 5). The Ionian Sea also presents a statistically significant increasing trend during the 2nd part of the future period (slope = $+0.9 \pm 0.4$ mm/year, $p = 0.046$; Table 5).

Contrastingly, a strong decreasing trend during the entire simulation period is identified for the SW Med (slope = -0.3 ± 0.1 mm/year, $p < 0.001$; Table 5), especially during the *Future Period* (slope = -0.3 ± 0.1 mm/year and $p = 0.026$); the storminess attenuation is supported by a decrease in storm maxima. Very low maxima also occur over the western-most Mediterranean, in the Alboran region (<30 cm), compared to the neighboring SW Med, but without a significant future trend ($p > a = 0.05$). In all the other regional seas, the annual sea level maxima range between 30 cm and 40 cm. The annual extremes do not show significant changes during the *Future Period* for most of the Mediterranean sub-basins; the majority of p-values support the hypothesis of no significant trend (high values), especially during the last 50 years of the 21st century. All coastal locations of the Adriatic Sea showed decreasing trends in local peak frequencies for the entire study period (*e.g.* Trieste; Fig. 4d), but, at the same time, higher annual sea level maxima may still appear in the *Future Period* (Figs. 4 c and 9). Although, the SLHs show an increasing tendency in the Tyrrhenian Sea during the mid *Past Period*, the extreme values drop significantly, especially during the first half of the 21st century, presenting an overall clear decreasing trend for the *Future Period* (slope = -0.5 ± 0.2 mm/year and $p = 0.003$; Table 5). The north-central Mediterranean Sea (Adriatic and Aegean Seas) shows a decreasing tendency of annual maxima over the first half of the *Future Period*, but

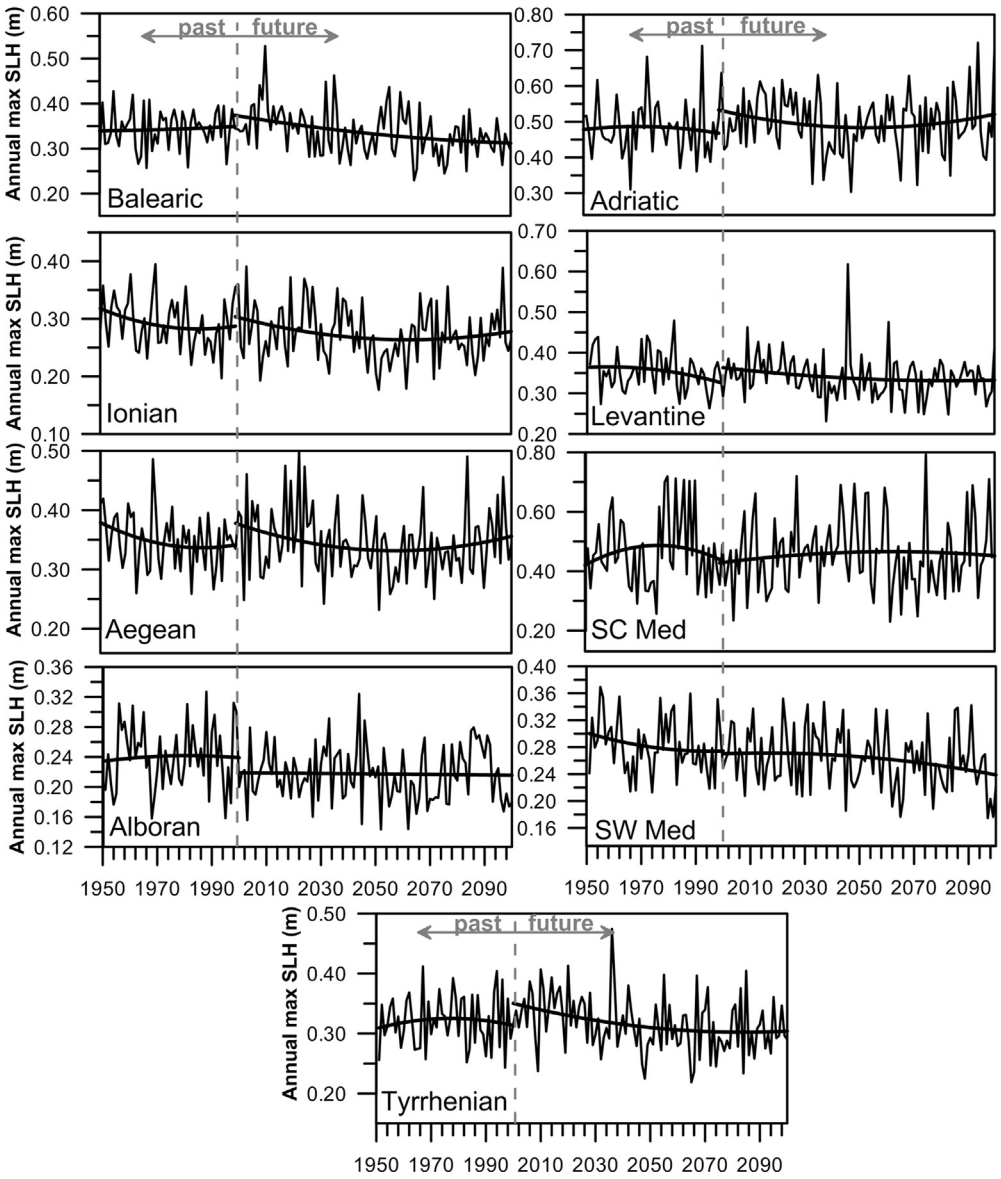

Fig. 9. Temporal evolution of annual maximum SLH (m) for the 9 regional seas of the Mediterranean (Fig. 1b); the 2nd degree polynomial trends of *Past* and *Future Periods* are indicated with solid black lines.

with a small increase during the last 50 years of the century (Fig. 9). It follows that the predicted attenuation of storminess refers more to the frequency of local peaks, duration and coverage of the storm surges and not to the magnitude of annual surge maxima, which is estimated to be higher than the peak values of the *Past Period*.

4.3. Evolution of seasonal variability

To investigate changes in the seasonal variability of storm surges in the Mediterranean, we calculated the occurrence frequency f (%) of annual SLH maxima per season, for all study locations, distinguishing between *Past* and *Future Periods* (Table 6). The difference between the two periods, $dif(\%) = 100 \times [(F - P)/P]$ is computed in order to show the potential relative contrast between past and future simulations for all locations; F and P correspond to *Future* and *Past Period* values of f (%). We also defined the corresponding monthly occurrence frequencies of SLH maxima at selected locations (Fig. 10); these locations cover the western (Barcelona, Alger and Marseille; Fig. 10a), central (Venice, Catania and Gabes; Fig. 10b) and eastern (Antalia, Hadera and Alexandria; Fig. 10d) Mediterranean, with the addition of three locations (Alexandroupolis, Chios and Iraklio; Fig. 10c) from the topographically complicated Aegean Sea.

Table 5
p-values and corresponding slopes (mm/yr) from linear regression analysis for each regional sea and each study period (past period, future period, 1st and 2nd 50-years spans of the future period, and the entire 150-year simulation period). The statistically insignificant trends are indicated with ns, which denotes no slope and is set for a confidence level of 90%; positive trends are shaded gray and statistically significant *p*-values are indicated with bold fonts.

	1951–2000		2001–2100		2001–2050		2051–2100		1951–2100	
	Past period		Future period		1st future period		2nd future period		All period	
	p-value	Slope	*p*-value	Slope	*p*-value	Slope	*p*-value	Slope	*p*-value	Slope
Adriatic	0.558	ns	0.460	Ns	**0.056**	-1.8 ± 0.8	0.900	ns	0.550	ns
Aegean	0.088	-0.8 ± 0.5	0.289	Ns	0.304	ns	0.091	-1.0 ± 0.5	0.137	ns
Alboran	0.973	ns	0.683	Ns	0.371	ns	0.304	ns	**0.009**	-0.2 ± 0.1
Balearic	0.616	ns	**0.001**	-0.6 ± 0.2	**0.004**	-1.4 ± 0.5	0.114	ns	**0.006**	-0.2 ± 0.1
Ionian	0.186	ns	0.247	Ns	0.821	ns	**0.046**	$+0.9 \pm 0.4$	**0.003**	-0.3 ± 0.1
Levantine	0.101	ns	**0.048**	-0.3 ± 0.2	**0.029**	-0.6 ± 0.6	0.725	ns	**0.010**	-0.2 ± 0.1
SC Med	0.960	ns	0.835	ns	**0.026**	$+2.3 \pm 1.0$	0.340	ns	0.970	ns
SW Med	0.141	ns	**0.026**	-0.3 ± 0.1	0.487	ns	0.146	ns	$<$**0.001**	-0.3 ± 0.1
Tyrrhenian	0.770	ns	**0.003**	-0.5 ± 0.2	**0.010**	-1.0 ± 0.5	0.973	ns	**0.035**	-0.2 ± 0.1

As expected, the majority of extreme events occur during winter and spring seasons for all locations. The western region is characterized by high occurrence frequencies of SLH during winter months. Especially for the Spanish and French coasts, the highest values (15–28%) are observed from December to March (Fig. 10a). Simulations showed an increase of winter and especially autumn frequencies together with a corresponding reduction of spring values for the *Future Period* (Barcelona, Nice, Marseille; Table 5) under the A1B scenario; for example, the autumn and spring relative differences for Barcelona are 450% and −32%, between *Past* and *Future Periods*, respectively.

North African locations (*i.e.* Tripolis, Gabes) present the highest spring and summer storm occurrences among the studied locations (Table 6). A striking feature is the monthly variability in Gabes (Fig. 10b), with the storm maxima concentrated in the period between February and May; the peak occurrence frequency in the station (29%) appears in May and is, by far, the highest spring value observed. These observations are in agreement with the findings of Trigo et al. (1999) climatology study of atmospheric cyclones in the Mediterranean region. They have found a pronounced increase of cyclone routes over northern Africa in spring, with major eastward and north-eastward paths. Regarding the future trends (Table 6), there seems to be a temporal shift of peak surges in the area, with an attenuation of the spring frequencies and higher possibility of summer storm surge events in the future; the simulation shows a 10% occurrence frequency of future summer peak SLHs, while the frequency was zero in the *Past Period.* Similar seasonal distribution is observed in Tripolis, where the spring frequencies are the highest among all locations for both *Past* and *Future Periods* (>63%, Table 6). In the eastern Mediterranean, storm events are expected to be most frequent from December to April (Fig. 10d), while relatively notable summer frequencies (∼2%) may also occur, mainly in the Levantine Sea; contrastingly, zero summer frequencies are derived for the majority of the locations, especially along the European coasts (Table 6).

High occurrence of annual maxima is predicted over the Adriatic coastal zone during winter and early spring, while relatively high autumn frequencies are also present, especially in the northern part (*e.g.* Trieste). During the *Future Period*, the spring ($dif_{\text{Venice}} = 15\%$ and $dif_{\text{Trieste}} = 100\%$) and autumn ($dif_{\text{Venice}} = 67\%$ and $dif_{\text{Trieste}} = 50\%$) frequencies increase in the northern part, with a related drop in winter frequencies ($dif_{\text{Venice}} = -10\%$ and $dif_{\text{Trieste}} = -22\%$). On the contrary, in the southern part of the area, a small increase of winter frequencies is observed (*e.g.* $dif_{\text{Dubrovnic}} = 3\%$). The locations of the Ionian Sea show similar temporal variability of surge events, with the majority of them occurring during winter and early spring (*e.g.* Catania; Fig. 10b). An increase of the possibility of significant spring surges is projected for the future conditions ($dif_{\text{Otranto}} = 40\%$ and $dif_{\text{Catania}} = 90\%$), accompanied by a reduction of the winter frequencies ($dif_{\text{Otranto}} = -16\%$ and $dif_{\text{Catania}} = -26\%$).

Differences are also observed between the North and South Aegean Sea (Fig. 10c). At the southern station of Iraklio, winter annual maxima are common (>25%), while the spring surge events are very few, compared to the northern stations of Chios and Alexandroupolis. Nevertheless, the majority of incidents occur during November and the following winter season (Table 6). Regarding future conditions, there is a general attenuation of autumn frequencies ($dif_{\text{Alexandroupolis}} = -50\%$, $dif_{\text{Kavala}} = -33\%$, $dif_{\text{Thessaloniki}} = -40\%$ and $dif_{\text{Iraklio}} = -63\%$). that is mostly accompanied by a small increase of the possibility of peak surges during spring (Table 6). However, the winter surges become more frequent over the central Aegean ($dif_{\text{Chios}} = 8\%$), while the related spring frequencies might be reduced ($dif_{\text{Chios}} = -16\%$).

Overall, we detected a probable general reduction of the winter storm frequencies over the Mediterranean region under the A1B scenario, and a mild increase of spring surges. It follows that our results show a possible temporal shift of surges in the annual cycle, accompanied by an increase of the temporal window of storm occurrence toward spring, findings that agree with Jordà et al. (2012) and Giorgi and Lionello (2008).

5. Discussion

In the present part of the paper, we discuss the spatio-temporal trends of maximum, average and statistically significant SLHs, together with the variability of statistically significant extreme events along the coastal zone of the entire Mediterranean, based on simulations of storm surge in the *Future Period* under A1B climate scenario. The discussion is based

Table 6
Seasonal percentage f (%) of maximum SLH occurrence at 28 study locations during Past (P) and Future (F) periods.[a] The difference percentage dif (%) = $100 \times [(F-P)/P]$ and the Mediterranean sub-region of each study station are also presented.[b]

	Station		Wi	Sp	Su	Au		Station		Wi	Sp	Su	Au
Alb	Ceuta	*P*	74	18	0	8	Adriatic	Venice	*P*	74	20	0	6
		F	71	23	0	6			*F*	67	23	0	10
		dif	−4	28	–	−25			dif	−9	15	–	67
Balearic	Barcelona	*P*	64	34	0	2		Ancona	*P*	62	26	0	12
		F	66	23	0	11			*F*	71	20	0	9
		dif	3	−32	–	450			dif	15	−23	–	−25
	Marseilles	*P*	70	26	0	4		Trieste	*P*	76	10	0	14
		F	68	22	0	10			*F*	59	20	0	21
		dif	−3	−15	–	150			dif	−22	100	–	50
	Nice	*P*	58	34	0	8		Zadar	*P*	70	20	0	10
		F	71	20	0	9			*F*	73	20	0	7
		dif	22	−41	–	13			dif	4	0	–	−30
	Genova	*P*	70	22	0	8		Dubrovnik	*P*	62	30	0	8
		F	69	25	0	6			*F*	64	26	0	10
		dif	−1	14	–	−25			dif	3	−13	–	25
	Ajaccio	*P*	60	28	0	12	Aegean	Iraklio	*P*	70	22	0	8
		F	76	19	0	5			*F*	72	25	0	3
		dif	27	−32	–	−58			dif	3	14	–	−63
Tyr	Naples	*P*	66	24	0	10		Thessaloniki	*P*	60	30	0	10
		F	73	22	0	5			*F*	62	32	0	6
		dif	11	−8	–	−50			dif	3	7	–	−40
SW Med	Alger	*P*	60	28	2	10		Kavala	*P*	64	24	0	12
		F	45	46	0	9			*F*	60	32	0	8
		dif	−25	64	−100	−10			dif	−6	33	–	−33
	Cagliari	*P*	52	38	0	10		Alexandroupolis	*P*	60	26	0	14
		F	63	32	0	5			*F*	60	33	0	7
		dif	21	−16	–	−50			dif	0	27	–	−50
SC Med	Tripoli	*P*	34	66	0	0		Chios	*P*	62	32	0	6
		F	32	63	3	2			*F*	67	27	0	6
		dif	−6	−5	–	–			dif	8	−16	–	0
	Gabes	*P*	8	86	0	6	Levantine	Antalia	*P*	66	22	4	8
		F	18	70	10	2			*F*	67	29	2	2
		dif	125	−19	–	−67			dif	2	32	−50	−75
Ionian	Catania	*P*	72	20	0	8		Mersin	*P*	66	24	4	6
		F	53	38	0	9			*F*	69	25	2	4
		dif	−26	90	–	13			dif	5	4	−50	−33
	Otranto	*P*	62	30	0	8		Hadera	*P*	70	24	0	6
		F	52	42	0	6			*F*	59	31	1	9
		dif	−16	40	–	−25			dif	−16	29	–	50
	Lefkada	*P*	58	32	0	10		Alexandria	*P*	72	24	2	2
		F	58	35	0	7			*F*	66	28	2	4
		dif	0	9	–	−30			dif	−8	17	0	100

[a] Winter, Spring, Summer and Autumn are indicated as Wi, Sp, Su, Au, respectively.
[b] Alb, Tyr, SW Med and SC Med are abbreviations of Alboran, Tyrrhenian, South-Western, and South-Central Mediterranean sub-regions, respectively.

on new results, focusing mainly on subjects not shown previously, while we also attempt a synthesis with existing knowledge.

5.1. General trends

The study period is divided in three 50-year time spans (one covering the *Past Period* and two from the *Future Period*), in order to investigate the general trends of the maximum and average SLH, under the A1B scenario. In addition, the minimum and average SLP of the three periods are also derived from the atmospheric climate simulation (RegCM3, see Section 2.1), in order to estimate the general trends of the extreme low and mean pressure levels during each 50-year period (Fig. 11). The related spatial variability of maximum and average SLH is presented in Fig. 12. Generally, the average SLHs over the entire Mediterranean Sea slightly decrease along the three 50-year periods (Fig. 12), following the mildly increasing trend of minimum SLPs (Fig. 11), which is probably related to the poleward shift of storm tracks and the reduction of cyclonic activity in an increasing CO_2 climate (Lionello et al., 2002). This is in agreement with the previously presented maximum SLH trends (Fig. 9 and Table 5), where we estimated decreasing trends in the majority of the regional Seas of the Mediterranean for the entire *Future Period*, of the order of −0.3 to −0.6 mm/year. Similar decreasing trends are reported by Jordà et al. (2012), who found general decreasing trends that are stronger during winter periods. However, distinctive deviations from this general trend occur at several regions and are discussed further down, especially concerning cases of potential appearance of extreme SLH events that may cause significant problems on the coastal zone.

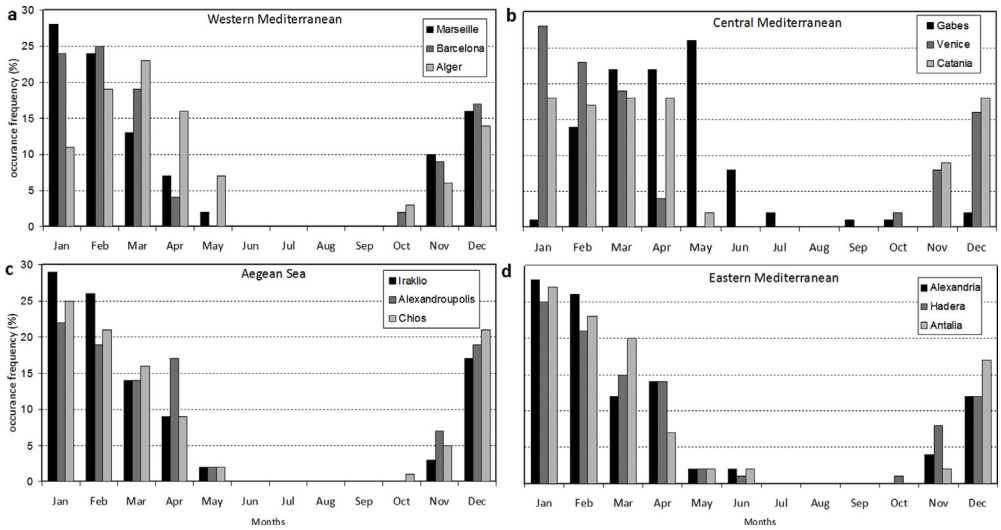

Fig. 10. Monthly occurrence frequency (%) of annual maximum SLH appearance, derived from the MECSM simulation under the future climatic scenario (2001–2100) at selected locations of the (a) Western Mediterranean, (b) Central Mediterranean, (c) Aegean Sea, and (d) Eastern Mediterranean.

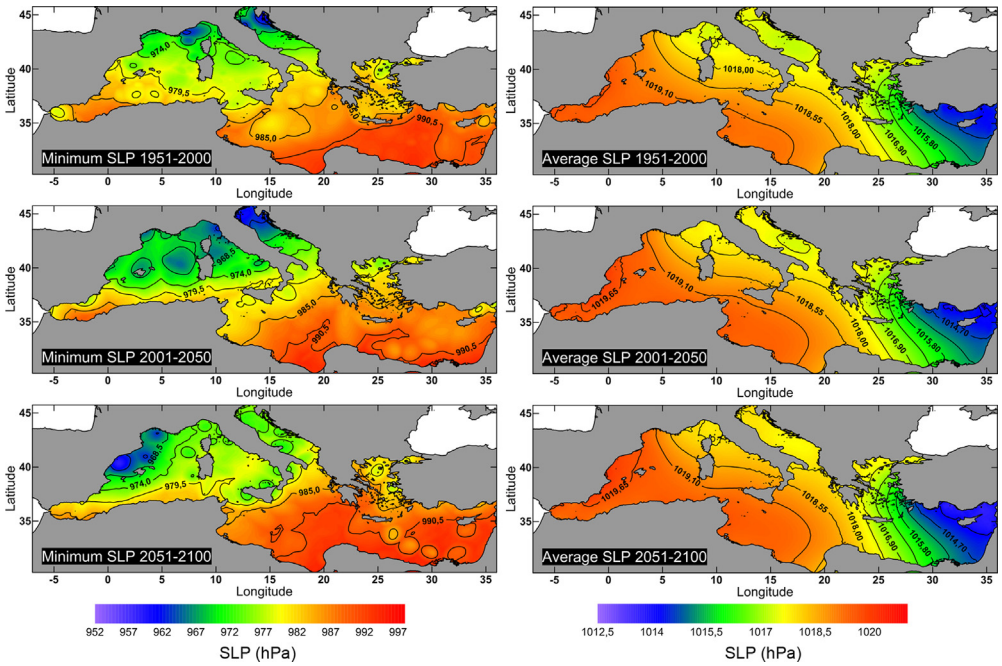

Fig. 11. Comparison of horizontal distributions of the absolute minimum (left) and the temporal mean (right) SLP (hPa) among the periods of 1951–2000, 2001–2050, and 2051–2100, as derived from the RegCM3 atmospheric fields.

The lowest pressure minima of the entire *Past Period* (∼960 hPa) appear over the N. Adriatic and Tyrrhenian Seas (Fig. 11). The minima are higher over the southern and eastern Mediterranean, especially over the Levantine basin (∼990 hPa). A large drop of low SLP (∼5.5 hPa) is predicted under the A1B scenario over the Balearic Sea in the first half of the 21st century. The levels are even lower during the following 50 years, especially along the Spanish and French coastline, corresponding to a decrease of around 6.5 hPa compared to the 1st part of the *Future Period*. In contrast, the simulated drop of pressure minima (<970 hPa) in the N. Adriatic Sea during the 2001–2050 period reverses during the 2051–2100 period, showing pressures higher than 970 hPa. There is a clear difference between the Balearic and Adriatic Seas, in relation to the minimum SLP

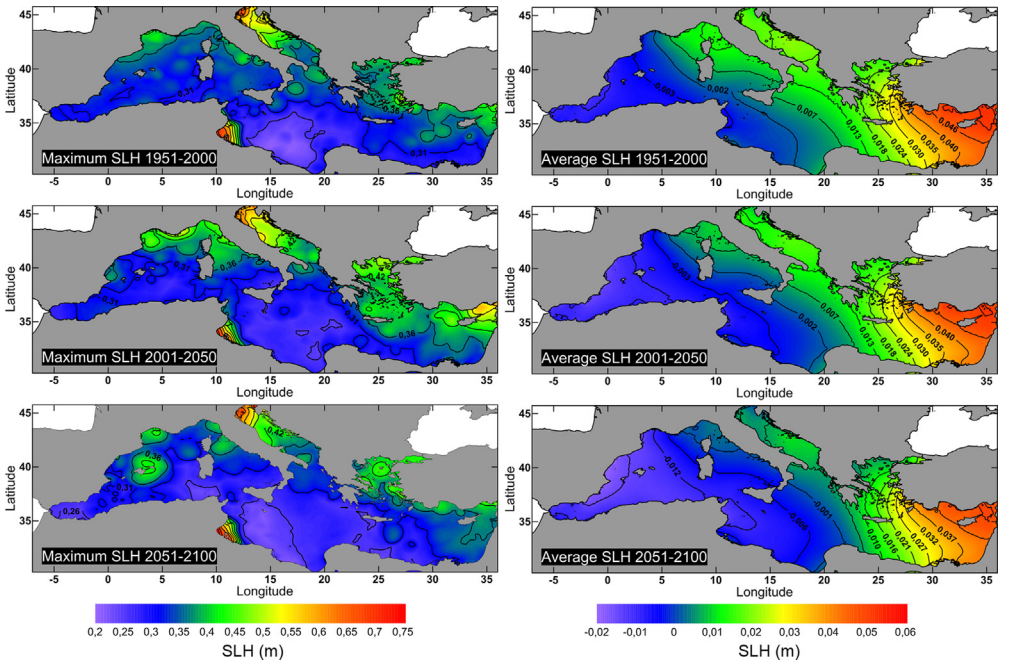

Fig. 12. Comparison of horizontal distributions of maximum (left) and average (right) SLH (m) among the periods of 1951–2000, 2001–2050, and 2051–2100, as derived from the MeCSM simulation.

appearance during these two future 50-year periods. The trends of low SLPs (Fig. 11) are reflected on the maximum SLH trends (Fig. 12), apart from the Spanish coasts. However, in the open Balearic Sea, we observe an area of increased peak SLHs along all 50-year periods, varying inversely with the corresponding SLP trends; the stronger low pressure systems in 2001–2050 cause a respective increase of maximum SLH values. Contrastingly, in the N. Adriatic Sea, the increasing trend of the SLH maxima presented in Fig. 9 (second half of the *Future Period*) does not follow the respective variation of the annual SLP minima, due to the control of winds on positive surges in the area (as discussed in Section 4); however, the expansion of low SLPs in the area impacts the SLHs the central and southern Adriatic region, with a significant southward increase of maximum SLHs (∼5–10 cm), compared to the *Past Period*. The Aegean Sea shows low SLH maxima during the *Past Period* and a pronounced increase in the entire region during 2001–2050 in agreement with the general average trends presented in Fig. 9; this increase, moderates in the second 50-year future period, under the A1B scenario. Over the northeastern Levantine coastal zone, the SLP minima of the first half of the 21st century decrease, initiating a corresponding increase of SLH maxima in the area. This is in agreement with Nissen et al. (2014), who found a statistically significant increase in the number of cyclones in the Levantine, under the A1B scenario. Over the entire basin, the results indicate that the maximum surges increase by around 3.5% in the 1st 50-year *Future Period*, compared to the *Past Period*. We also estimated a decrease of surge maxima by an average of −7% for 2051–2100, compared to 2001–2050.

Regarding the spatio-temporal trends of mean SLHs (Fig. 12, right panels) we see a similar variability to the mean SLP fields, with a distinct eastward increase of nominal sea levels. The general attenuation of storminess over the eastern Mediterranean basin under the A1B scenario is reflected in these results with a reduction of average SLHs throughout the 21st century (of the order of −17% and −5% for the 1st and 2nd parts of the *Future Period*, respectively). The general decrease

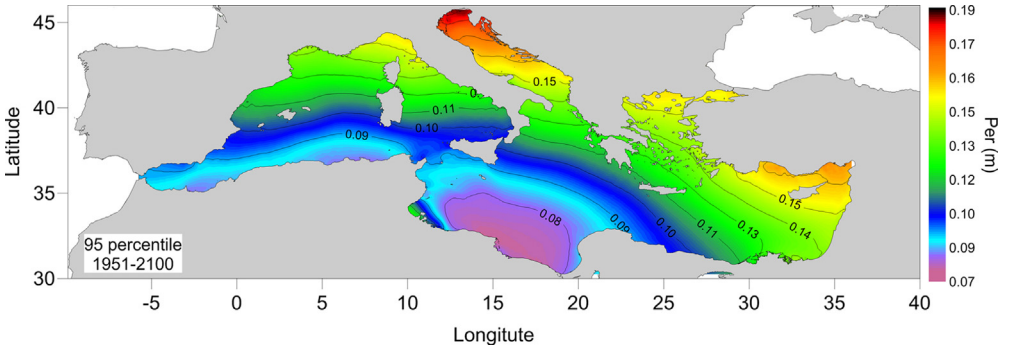

Fig. 13. Horizontal distribution of the 95th percentile for SLH (m) over the Mediterranean region, covering the entire future period (2001–2100).

of surges under the A1B scenario is shown in many similar climatic modeling works, like Conte and Lionello (2013) , who showed a 5% decrease of positive and negative surges in the 21st century and Marcos et al. (2011), who found a decrease in the average number of surges and related return levels over the Mediterranean. This attenuation is probably related to the increase of winter SLPs, also supported by Jordà et al. (2012) and Giorgi and Lionello (2008) ; our results also show a temporal shift of surges, with increase of spring and mild increase of summer values, especially in the Eastern Mediterranean and Adriatic (Fig. 10 and Table 6), which is consistent with the increase in the amplitude of the seasonal cycle, found by Jordà et al.

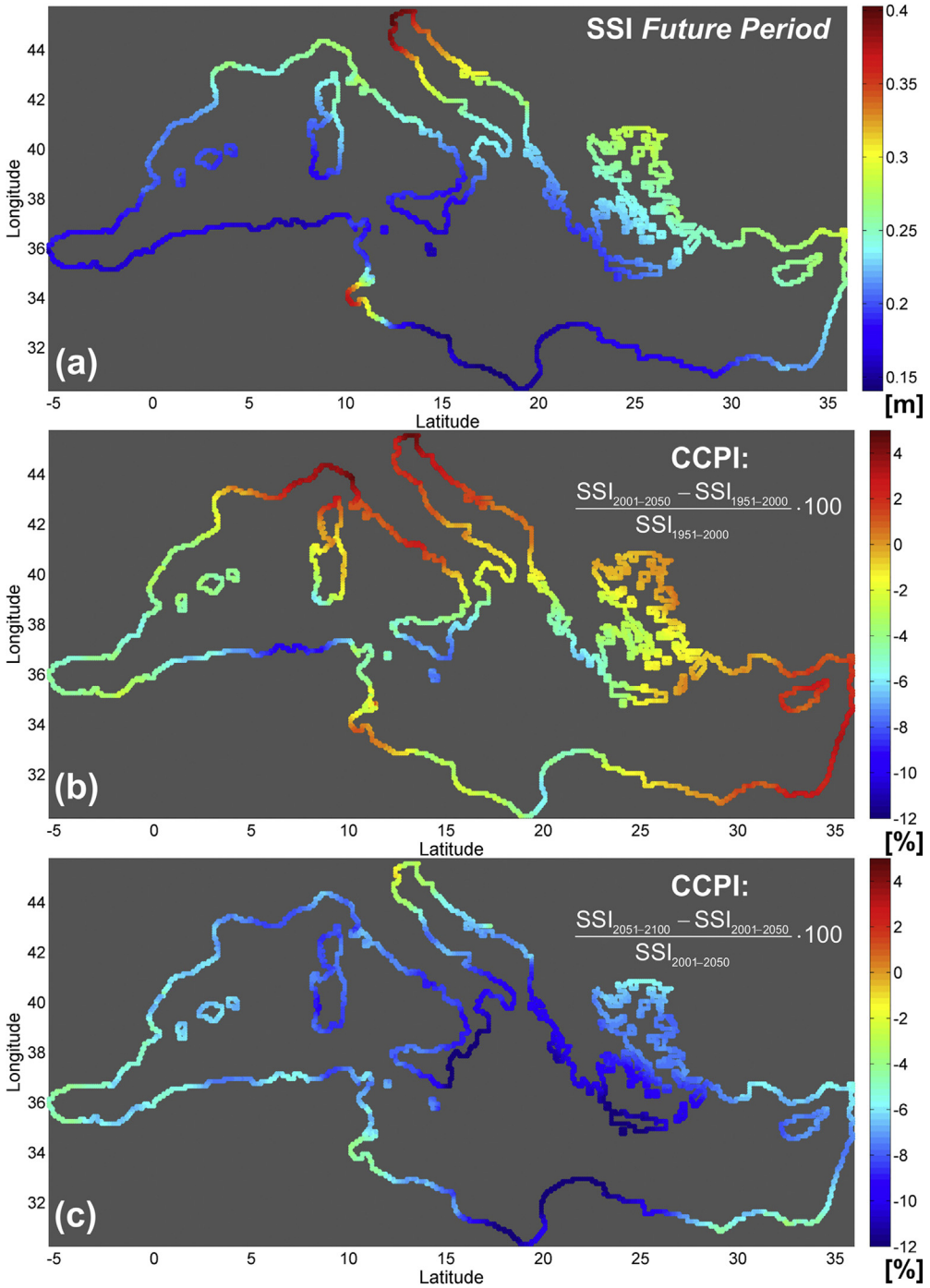

Fig. 14. (a) Storm Surge Index (*SSI*, in m) along the entire Mediterranean coastline as derived from the future 100-year MeCSM simulation, (b) Climate Change Percent Index (*CCPI*) values between the 1st 50-year period of the 21st century and the *Past Period*, and (c) between the 1st and 2nd 50-year spans of the *Future Period*.

(2012). However, our results show that, even though peak SLHs show decreasing future trends over the entire basin, under the A1B scenario, higher surges can be expected locally in the 1st part of the 21st century, compared to the *Past Period*; these relatively stronger events are identified in the Balearic (45–53 cm over 40 cm in the *Past Period*), Aegean (45–50 cm over 45 cm in the *Past Period*), and Tyrrhenian (40–48 cm over <40 cm in the *Past Period*) Seas (Fig. 9). At the same time, the durations of storms also show a decreasing future tendency (Fig. 8), yet during the 1st part of the 21st century we find higher duration values, compared to the preceding and following periods over the eastern Mediterranean and the Balearic and Tyrrhenian Seas. It follows that our results show that, even though the general trends agree with the general attenuation of storminess in the Mediterranean under the A1B scenario, it is likely that higher and longer surge events can still appear in certain parts of the basin.

The distribution of the 95th percentile for the entire study period (1951–2100) over the Mediterranean confirms the high SLH levels over the N. Adriatic Sea, where 5% of the values may noticeably exceed the level of 17 cm (Fig. 13), in agreement with the highest annual maximum SLHs obsreved over the region (Fig. 12). Contrastingly, the central southern region reveals the lowest high-order percentiles (<8 cm) of SLH, with an exception over the gulf of Gabes (>10 cm). Similar to the distribution of the annual maximum SLHs (Fig. 12), the central N. Aegean and the northeastern Levantine appear to give lower high-order percentiles of SLH, compared to the N. Adriatic, but higher than the rest of the Mediterranean Sea, where high- order percentiles range around 15 cm. A rather obvious borderline that coincides with the 10 cm contour line travels along the Balearic Islands, Sicily, Crete, and crosses transversely the Egyptian coastline (Fig. 13). This can be seen as an implicit boundary, which divides the region into two separate areas with low (southwest) and high (northeast) 95th percentile levels for SLH.

5.2. Variability of extreme events along the Mediterranean coastline

The statistically significant maximum SLH that may occur for the period of 2001 to 2100 under the specific climatic scenario can be described by *SSI* (see Section 3.2). The *SSI* values along all coastal grid cells are calculated for the entire *Future Period* and presented in Fig. 14, showing the distribution of the potential annual maximum SLH for a 100- year period along the Mediterranean coastline. The lower panels in Fig. 14 show the relative differences between the 1st 50-year period of the 21st century and the *Past Period* (Fig. 14b), and between the 1st and 2nd 50-year spans of the *Future Period* (Fig. 14c); this parameter is defined as the Climate Change Percent Index by Conte and Lionello (2013) , a naming convention which we follow here, abbreviated as: *CCPI*.

The spatial trends follow the observations made for each particular coastal region in the preceding discussion. The highest future *SSIs* (Fig. 14a) are detected in the N. Adriatic, especially over the Venice Lagoon (∼38 cm), at the Gulf of Gabes (>35 cm), along the French, western Italian, N. Aegean, and Minor Asia coasts (∼30–25 cm), and in the eastern Levantine (∼25–30 cm). The entire coastline of Cyprus shows *SSI* values over the mean Mediterranean level (SSI_{mean} = 22 cm), while, for most of the central and eastern European coasts, the *SSIs* range above the mean level; only the areas of South Italy, the Balearic Islands, western Corsica, western Sardinia, Malta, the southern Ionian Sea and southern Crete present lower values, along with the entire African coastline, with the exception of Gabes. Again, as in the 95th percentiles of SLHs, we see the same 'boundary', at an angle of around 30° (clockwise) with the parallels, dividing the region to low and high atmospheric storm-induced accumulation of waters. Our results show the same spatial distribution of high and low *SSI* along the coastal zone of the Mediterranean as Conte and Lionello (2013; their Fig. 7). In terms of *SSI* values the results of Conte and Lionello (2013) present high variability on peak values (∼15–25 cm), namely in the N. Adriastic and the gulf of Gabes. In these areas, we find that our results correlate well with the lowest *SSI* future projections, whereas in all other areas of the coastal zone our results are in good agreement.

Regarding the *CCPI* values, the results show that there is a general decrease in the period of 2001–2050 (Fig. 14b), ranging from −2 to −10% in the western part of the western Mediterranean and from 0 to −9% in the central part of the basin; however, an increase in the mean *SSI* values, of the order of 1–4%, exists along the entire Adriatic, Levantine, Tyrrhenian and eastern Balearic Seas. Toward the end of the 21st century (Fig 4c) a generalized decrease of *SSIs* is observed throughout the basin (compared to the preceding period). This finding agrees with the general distribution of the annual maximum SLHs presented in Fig. 12. This reduction is lower in the N. Adriatic (∼−2%), especially along the Venice lagoon, where higher maximum SLH may appear during the 2051-2100 period (Fig. 12), and strongest in the central Mediterranean (∼−12% for S. Italy and Lybia); the western and eastern parts of the basin exhibit a relative decrease of the order of −4 to −8%.

6. Concluding remarks

In the present study we investigated the evolution and characteristics of storm surge events in the Mediterranean Sea due to future atmospheric conditions under climate change. The study was based on the A1B climate scenario and covered the Mediterranean basin for a period of 150 years (1951–2100). *In situ* observations confirmed the good performance of the storm surge climate simulations for several regions of the Mediterranean Sea. Additional hindcast results, presented in Appendix A, showed a good agreement between hindcast and climatic runs.

The investigation of the atmospheric driving factors (wind and pressure) revealed significant differences regarding their contribution on the appearance of strong surge events in the sub-regions of the Mediterranean. The relation of the coastline morphology and orientation with the wind direction affects the wind-driven sea level changes over coastal areas. However,

uncertainties in our climatic projections exist and involve the omission of steric effects, tides, sea level rise and the mass inflow of Atlantic waters that were not taken into account in our numerical simulations; furthermore, uncertainties regarding the input atmospheric data are always a concern in storm surge modeling. Moreover, other characteristics such as the thermohaline circulation, especially changes in the connectivity with Atlantic Ocean (Bryden et al., 1994) and the important buoyant input from Black Sea (Androulidakis et al., 2012). The latter, combined with the increase of mean sea level and additional land subsidence (Conte and Lionello, 2013), may also contribute on different patterns of the sea level variability under potential climate change conditions. On the other hand, the effect of sea level rise does not necessarily change our solution, since it could be superimposed to the simulated SLHs, without any significant error. The steric effects are also expected to have minimal impact to simulated surges in the coastal zone, since the impact is higher in the open sea and low in coastal areas (Tsimplis et al., 2008). Regarding tides, the possibility of surges coinciding with high water would mean that our solution can underestimate surge levels in areas with significant tidal signals (*e.g.* N. Adriatic). The mass inflow through the Gibraltar strait is expected to influence mainly the westernmost part of the basin; the high underestimation of measured *SLH*s in Ceuta by MeCSM is most likely due to this omission, but the impact is localized and the model performs well in all other areas. Overall, the agreement of the control run with *in situ* data and hindcast results shows that MeCSM effectively describes the SLH variability of the Mediterranean in the present climate, and, therefore, adds confidence to the A1B climatic storm surge projections. The combination of storm surges, mass exchanges, wave set-up and astronomical tides (not examined in this paper) may significantly increase the risk of inundation over the Mediterranean coastal region. Therefore the investigation of these combined effects under climate change conditions is a useful and important task for the coastal management and protection.

Our investigation of the Mediterranean surges controlled by wind and/or SLP, confirms previously reported findings and elaborated further on scarcely studied regions, like the Aegean Sea. In agreement with other related work (*e.g.* Orlić et al., 1994; Pirazzoli and Tomasin, 2002; Conte and Lionello, 2013; Krestenitis et al., 2011), we found that in the N. Adriatic Sea extreme events are controlled by the strong southeasterly winds, while, the nominal sea level variability is affected mainly by pressure. Strong surges in the Gulf of Gabes are also wind-driven, mainly under predominance of easterly winds, combined with the presence of an extended continental shelf. The coastal zone of Alexandria is another area with relatively high influence of the most frequent northerly winds on SLHs. On the other hand, the accumulation of waters near the shore due to direct wind effect is of lower influence on the storm surge magnitude in most Mediterranean areas (Balearic, Tyrrhenian, S. Adriatic and eastern Mediterranean), compared to the direct impact of low pressure systems. Along the Balearic coastline (French and Spanish coasts), the control of SLP over the storm surge extremes is pronounced in the western part of the northern coasts, with lower contribution of winds (unfavorable wind directions – low frequency of southerly winds). The N. Aegean Sea is characterized by a strong impact of pressure gradients, combined with an increasing impact of winds toward the east due to the different topographic features along its northern coastal zone. In general, the Aegean Sea presents a smaller dependence of average SLHs by the wind forcing, compared to the other regions of the eastern basin. This is most likely linked to the topography of the archipelago, namely the large number and the irregular setting of islands.

Regarding future trends, we found that the surge extremes over the entire Mediterranean region may decrease, in agreement with Conte and Lionello (2013) and Marcos et al. (2011); this attenuation is probably related to the increasing trend of the minimum sea level pressures (Nissen et al., 2014; Jordà et al., 2012; Šepić et al., 2012; Giorgi and Lionello, 2008). We showed that another contributing factor for the expected attenuation of storminess under the A1B scenario is the predicted attenuation of the wind contribution to the storm surge frequencies. Our results show a general reduction of the winter storm surge frequencies. Moreover, we found a temporal shift of surges, with increase of spring and mild increase of summer values, especially in the Eastern Mediterranean and the Adriatic, which is consistent with Jordà et al. (2012), Tsimplis and Shaw (2010) and Marcos and Tsimplis (2007). Similarly, the autumn extremes may be more common under the A1B future scenario over the Adriatic region, due to the higher occurrence frequencies of southerly winds during autumn. A clear attenuation of the occurrence frequency for spring extreme events is predicted based on simulations over the central Aegean Sea. For the North African coasts we have estimated an attenuation of spring extreme surges, with higher possibility of summer events.

Even though the surge extremes show a likely decreasing trend in the entire basin, in terms of surge heights, coverage and duration, consistent with the general attenuation of storminess under A1B, we have found that higher surges, compared to the past climate, can still be expected in regional seas, like the eastern Mediterranean and the Adriatic, Balearic and Tyrrhenian Seas, in the first part of the 21st century (2001–2050). Especially in the southern part of the Adriatic, a southward expansion of pressure-driven surges is predicted. An increase of 1–4% of statistically significant surges in these areas is calculated from our simulation, combined with higher storm duration values during the first 50 years of the A1B scenario. This is in agreement with Šepić et al. (2012), who argue that although the average sea level variability is expected to decrease in the future, the extreme sea levels for these period bands will not decrease. In the following period (2051–2100), the surge extremes are estimated to decrease in the entire basin. Thus, our results show that the storminess attenuation, under A1B future climatic conditions, is more related to a decrease in duration, coverage and local peak frequency of storm surges and actually not to the magnitude of extreme events.

The spatial variability of extreme surges does not show significant changes in the future projections, while it should be noted that the aforementioned attenuation of surges toward the end of the 21st century is minimal in the N. Adriatic ($<-2\%$), compared to the rest of the basin (-4 to -12% reduction of *CCPI*s). Finally, calculated percentiles of *SLH*s and coastal *SSI*s show

that a type of 'implicit boundary' exists in the basin that divides it in two separate areas with low (southwest) and high (northeast) surge levels.

Acknowledgements

This research has been co-funded by the European Union (European Social Fund—ESF) and Greek National Funds through the Operational Program "Education and Lifelong Learning" of the National Strategic Reference Framework (NSRF) —Research Funding Program: "THALES. Investing in knowledge society through the European Social Fund" under the Project "CCSEAWAVS". The authors are grateful to Y. Tegoulias, C. Anagnostopoulou and K. Tolika (Department of Meteorology and Climatology, Aristotle University of Thessaloniki) for kindly providing the atmospheric fields produced by the RegCM3 model and used as forcing input for the storm surge simulations, carried out in this study. The authors would also like to acknowledge the kind provision of tide-gauge data, located in the Aegean and the Ionian Seas, by the Hellenic Navy Hydrographic Service (HNHS).

Appendix A.

Comparison between hindcast and climatic storm surge simulations

In the present section, we compare the results of the climatic simulation of MeCSM to hindcast simulations, which are also based on the same hydrodynamic model, namely AUTSSM (De Vries et al., 1995; Krestenitis et al., 2011; Trifonova et al., 2012; Villatoro et al., 2014), covering the period of 2000–2004. This hindcast simulation was developed in the framework of the E.U. project CORI: «Prevention and management of sea originated risks to the coastal zone», INTERREG IIIB/ARCHIMED

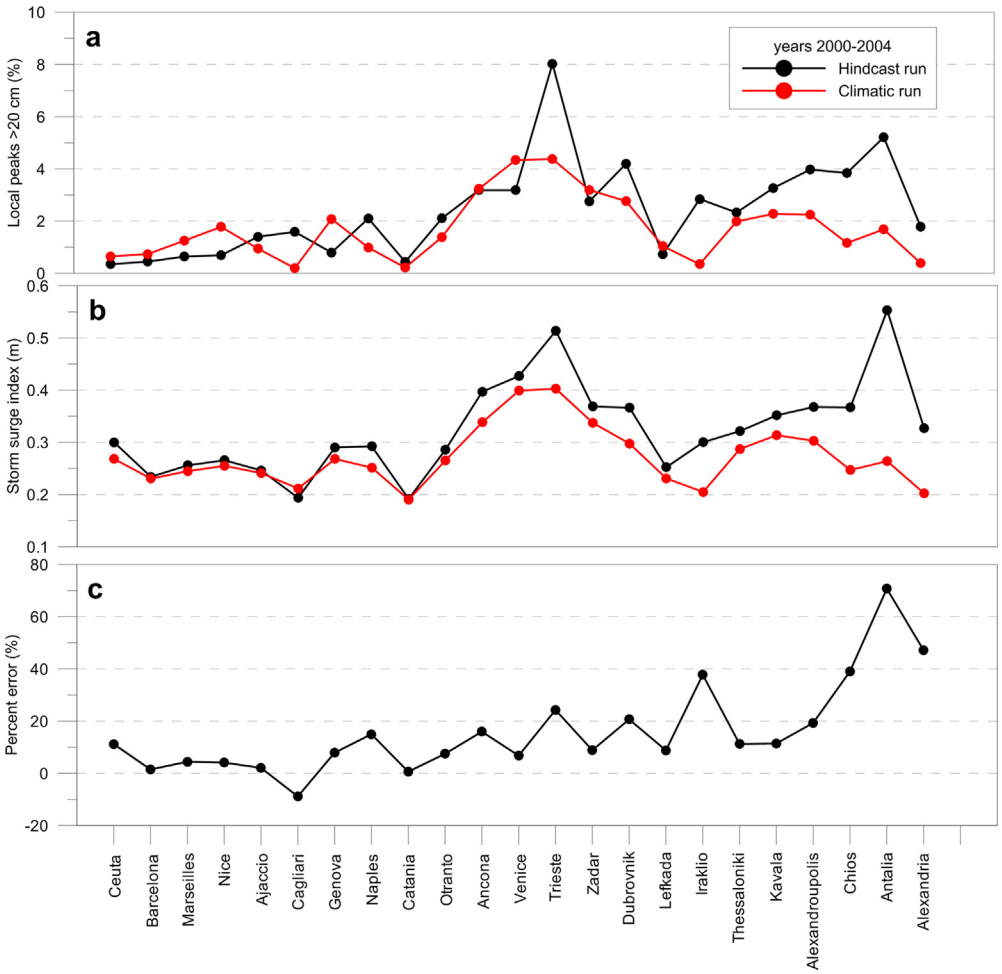

Fig. A1. (a) Number of SLH local peaks that exceed 20 cm, (b) Storm Surge Index (*SSI*) and (c) Percent Error (%) at 23 Mediterranean locations (east to west) from hindcast (black) and climatic (red) runs for the 2000–2004 period. (For interpretation of the references to color in this figure legend, the reader is referred to the web version of this article.)

and its performance over the Mediterranean region has been previously tested and validated by Krestenitis et al. (2011). The hindcast realistic simulations were executed with the same barotropic hydrodynamic model and set-up and, therefore, the comparison between the two simulations (hindcast and control) can be used to examine the reliability of the modeling system. The main difference between the two simulations is that the realistic simulation is forced with data-assimilated SLP and wind fields from the operational forecasting system POSEIDON (http://poseidon.hcmr.gr/; Papadopoulos et al., 2002). The period of 2000–2004 (early 21st century) is considered appropriate for the evaluation of the climatic control run because it covers both control run period and very early future scenario run, as mentioned in Section 2.3.

The local peaks that exceed the 20 cm threshold for 23 Mediterranean locations (Fig. 1c) were derived from both simulations (Fig. A1). The realistic simulation, forced with meteorological data, computed more peaks that exceed the 20 cm level for the majority of the locations. However, both models show a similar spatial variation of local maxima, presenting the highest number of local peaks over the central region and especially in the N. Adriatic Sea (*i.e.* Trieste and Venice). High SLH values are also detected in the Aegean Sea, while the fewest local maxima are observed along the Balearic coastline; the area from Ceuta to Catania shows frequencies of local peaks over 20 cm that are lower than 2% (Fig. A1a). For Barcelona, Marseille and Nice, no local peaks exceed the 30 cm threshold in both simulations (not shown). Both models reproduced the largest number of local peaks over 20 cm in Trieste (>4%; Fig. A1a). Contrastingly, the lowest number of peaks over the north-central Mediterranean is derived over south Italy (Catania) by both models. In almost all N. Aegean locations, SLHs over 20 cm range between 2% and 4%. A notable difference between the two simulations is observed in Antalia (south Turkey), where the realistic simulation produced a significantly higher number of local peaks, compared to the simulation under the climatic scenario. However, both simulations showed that north Levantine Sea (Antalia) reveals more peak SLHs than south Aegean Sea (Iraklio, Chios) and south Levantine Sea (Alexandria). At the same time, west to east spatial variability is similar for both simulations, confirming the good performance of the climate simulations, in spatial terms, during the examined period.

The *SSI* for the 5-year period was also calculated, in order to estimate the sea level anomalies from both simulations. The performance of the MeCSM simulation is tested based on the *SSI* difference from the realistic simulation at the previously discussed 23 locations (Fig. A1b). These values were also used to calculate the Percent Error (E) between the two simulations (Fig. A1c); this error is calculated subtracting the climate scenario results from the hindcast results, and is therefore positive when the climate simulation predicts lower *SSIs* than the hindcast simulation. The climate simulation shows good performance over the west and central Mediterranean, where the two SSIs are almost equal for all locations. Small but notable differences occur over the N. Adriatic, where similarly to the local peak frequencies, the hindcast shows higher surges (*e.g.* Trieste). However, the N. Adriatic climatic *SSIs* for the 2000–2004 period are closer to the ones calculated from the observed time-series, as presented for Trieste in Fig. 2a, indicating the good performance of the MeCSM model for the period in question. The differences are smaller over the Ionian (*i.e.* Lefkada) and N. Aegean (*i.e.* Thessaloniki, Kavala, Alexandroupolis) Seas; the highest annual values of the MeCSM simulation range around 30 cm, while the hindcast ones are slightly higher (∼35 cm). The increasing spatial trend from South to North Aegean is similar in both simulations. Contrastingly, the climatic simulation produces significantly lower values for the north Levantine area (*e.g.* Antalia), where the difference between the two *SSIs* is about 30 cm. Therefore, the Percent Error has the highest values at Antalia (∼60%), while far lower differences (<20%) were computed for the central and western Mediterranean region (Fig. A1c). However, that the SLH in the north Levantine basin is higher in both simulations, compared to the southern station of Alexandria and the stations of Chios and Iraklio to the west.

References

Androulidakis, Y., Krestenitis, Y., Kourafalou, V., 2012. Connectivity of north aegean circulation to the black sea water budget. Cont. Shelf Res. 48, 8–26.

Bengtsson, L., Hodges, K.I., Roeckner, E., 2006. Storm tracks and climate change. J. Clim. 9 (15), 3518–3543.

Bondesan, M., Castiglioni, G.B., Elmi, C., Gabbiabelli, G., Marocco, R., Pirazzoli, P.A., Tomasin, A., 1995. Coastal areas at risk from storm surges and sea-level rise in northeastern italy. J. Coastal Res. 11 (4), 1354–1379.

Bryden, H., Candela, J., Kinder, T.H., 1994. Exchange through the strait of gibraltar. Prog. Oceanogr. 33, 201–248.

Calafat, F.M., Jordà, G., Marcos, M., Gomis, D., 2012. Comparison of mediterranean sea level variability as given by three baroclinic models. J. Geophys. Res. 117, C02009. doi:http://dx.doi.org/10.1029/2011JC007277.

Campins, J., Genovés, A., Picornell, M.A., Jansà, A., 2011. Climatology of mediterranean cyclones using the ERA-40 dataset. Int. J. Climatol. 31 (11), 1596–1614.

Camuffo, D., Secco, C., Brimblecombe, P., Martin-Vide, J., 2000. Sea storms in the adriatic sea and the western mediterranean during the last millennium. Clim. Change 46 (1–2), 209–223.

Carillo, A., Sannino, G., Artale, V., Ruti, P.M., Calmanti, S., Dell'Aquila, A., 2012. Steric sea level rise over the mediterranean sea: present climate and scenario simulations. Clim. Dyn. 39 (9–10), 2167–2184.

Conte, D., Lionello, P., 2013. Characteristics of large positive and negative surges in the mediterranean sea and their attenuation in future climate scenarios. Glob. Planet. Change 111, 159–173.

Cox, D.T., Kobayashi, N., 2000. Identification of intense, intermittent coherent motions under shoaling and breaking waves. J. Geophys. Res.: Oceans (1978–2012) 105 (C6), 14223–14236.

Criado-Aldeanueva, F., Del Río Vera, J., García-Lafuente, J., 2008. Steric and mass-induced mediterranean sea level trends from 14 years of altimetry data. Glob. Planet. Change 60 (3), 563–575.

Davis, N., Bowden, J., Semazzi, F., Xie, L., Önol, B., 2009. Customization of RegCM3 regional climate model for Eastern Africa and a Tropical Indian Ocean domain. J. Clim. 22 (13), 3595–3616.

De Vries, H., Breton, M., de Mulder, T., Krestenitis, Y., Ozer, J., Proctor, R., Voorrips, A., 1995. A comparison of 2D storm surge models applied to three shallow european seas. Environ. Softw. 10 (1), 23–42.

Fritsch, J.M., Chappell, C.F., 1980. Numerical prediction of convectively driven mesoscale pressure systems. part ii. mesoscale model. J. Atmos. Sci. 37 (8), 1734–1762.

Giorgi, F., 2006. Climate change hot- spots. Geophys. Res. Lett. 33 (8), L08707. doi:http://dx.doi.org/10.1029/2006GL025734.

Giorgi, F., Lionello, P., 2008. Climate change projections for the mediterranean region. Glob. Planet. Change 63, 90–104.

Giorgi, F., Marinucci, M.R., Bates, G.T., 1993a. Development of a second-generation regional climate model (RegCM2). Part I: boundary-layer and radiative transfer processes. Mon. Weather Rev. 121 (10), 2794–2813.
Giorgi, F., Marinucci, M.R., Bates, G.T., De Canio, G., 1993b. Development of a second-generation regional climate model (RegCM2). Part II: convective processes and assimilation of lateral boundary conditions. Mon. Weather Rev. 121 (10), 2814–2832.
Grell, G.A., 1993. Prognostic evaluation of assumptions used by cumulus parameterizations. Mon. Weather Rev. 121 (3), 764–787.
Gualdi, S., Somot, S., Li, L., Artale, V., Adani, M., Bellucci, A., Braun, A., Calmanti, S., Carillo, A., Dell'Aquila, A., Deque, M., Dubois, C., Elizalde, A., Harzallah, A., Jacob, D., L'Heveder, B., May, W., Oddo, P., Ruti, P., Sanna, A., Sannino, G., Scoccimarro, E., Sevault, F., Navarra, A., 2013. The circe simulations: regional climate change projections with realistic representation of the Mediterranean Sea. Bull. Am. Meteorol. Soc. 94 (1), 65–81.
Holtslag, A.A.M., Moeng, C.H., 1991. Eddy diffusivity and countergradient transport in the convective atmospheric boundary layer. J. Atmos. Sci. 48 (14), 1690–1698.
IPCC, 2001. Climate Change, The Scientific Basis. Cambridge University Press, pp. 881.
Jaffe, B., Sallenger, A., 1992. The contribution of suspension events to sediment transport in the surf zone. Proceedings of the 23rd International Coastal Engineering Conference 3, Am. Soc. Civ. Eng., New York, pp. 2680–2693.
Jordà, G., Gomis, D., Alvarez-Fanjul, E., Somot, S., 2012. Atmospheric contribution to mediterranean and nearby atlantic sea level variability under different climate change scenarios. Glob. Planet. C 80–81, 198–214.
Kendall, M.G., 1975. Rank Correlation Methods, 4th ed. Charles Griffin, London.
Krestenitis, Y.N., Androulidakis, Y.S., Kontos, Y.N., Georgakopoulos, G., 2011. Coastal inundation in the north-eastern Mediterranean coastal zone due to storm surge events. J. Coastal Conservation 15 (3), 353–368.
Lionello, P., Dalan, F., Elvini, E., 2002. Cyclones in the mediterranean region: the present and the doubled CO∼2 climate scenarios. Clim. Res. 22, 147–159.
Lionello, P., Cavaleri, L., Nissen, K.M., Pino, C., Raicich, F., Ulbrich, U., 2012a. Severe marine storms in the northern Adriatic: characteristics and trends. Phys. Chem. Earth Parts A/B/C 40, 93–105.
Lionello, P., Galati, M.B., Elvini, E., 2012b. Extreme storm surge and wind wave climate scenario simulations at the venetian littoral. Phys. Chem. Earth 40–41, 86–92.
Lionello, P., Boldrin, U., Giorgi, F., 2008a. Future changes in cyclone climatology over europe as inferred from a regional climate simulation. Clim. Dyn. 30 (6), 657–671.
Lionello, P., Cogo, S., Sanna, A., 2008b. The mediterranean surface wave climate inferred from future scenario simulations. Global Planet. Change 63, 152–162.
Lionello, P., Giorgi, F., 2007. Winter precipitation and cyclones in the mediterranean region: future climate scenarios in a regional simulation. Adv. Geosci. 12, 153–158.
Lionello, P., Malanotte-Rizzoli, P., Boscolo, R., Alpert, P., Artale, V., Li, L., Xoplaki, E., 2006. The mediterranean climate: an overview of the main characteristics and issues. Dev. Earth Environ. Sci. 4, 1–26.
P. Lionello, 2005. Extreme storm surges in the gulf of venice: Present and future climate. In: Flooding and Environmental Challenges for Venice and Its Lagoon: State of Knowledge, edited by CA Fletcher, and T. Spencer, pp. 59–69.
Lionello, P., Nizzero, A., Elvini, E., 2003. A procedure for estimating wind waves and storm-surge climate scenarios in a regional basin: the adriatic sea case. Clim. Res. 23 (3), 217–231.
Lowe, J.A., Gregory, J.M., 2005. The effects of climate change on storm surges around the United Kingdom. Philos. Trans. R. Soc. A: Math. Phys. Eng. Sci. 363 (1831), 1313–1328.
Mann, H.B., 1945. Non-parametric tests against trend. Econometrica 13, 163–171.
Marcos, M., Jordà, G., Gomis, D., Pérez, B., 2011. Changes in storm surges in southern europe from a regional model under climate change scenarios. Glob. Planet. Change 77 (3), 116–128.
Marcos, M., Tsimplis, M.N., 2007. Variations of the seasonal sea level cycle in southern europe. J. Geophys. Res. Oceans (1978–2012) 112, C12.
Marcos, M., Tsimplis, M.N., Shaw, A.G., 2009. Sea level extremes in southern europe. J. Geophys. Res. Oceans (1978–2012) 114, C1. doi:http://dx.doi.org/10.1029/2008JC004912.
Mavromatis, T., Stathis, D., 2011. Response of the water balance in greece to temperature and precipitation trends. Theor. Appl. Climatol. 104, 13–24.
Nicholls, R.J., 2006. Storm surges in coastal areas. natural disaster hotspots: case studies. Disaster Risk Manage. 6, 79–108.
Nissen, K.M., Leckebusch, G.C., Pinto, J.G., Uwe Ulbrich, U., 2014. Mediterranean cyclones and windstorms in a changing climate. Reg. Environ. Change 14 (5), 1873–1890.
Nicholls, R.J., Hoozemans, F.M.J., 1996. The mediterranean: vulnerability to coastal implications of climate change. Ocean Coastal Manage. 31 (2-3), 105–132.
Onoz, B., Bayazit, M., 2003. The power of statistical tests for trend detection. Turk. J. Eng. Environ. Sci. 27, 247–251.
Orlić, M., Kuzmić, M., Pasarić, Z., 1994. Response of the adriatic sea to the bora and sirocco forcing. Contin. Shelf Res. 14 (1), 91–116.
Ozturk, T., Altinsoy, H., Türkeş, M., Kurnaz, M.L., 2012. Simulation of temperature and precipitation climatology for the central asia cordex domain using RegCM 4.0. Clim. Res. 52, 63–76.
Pal, J.S., et al., 2007. Regional climate modeling for the developing world: the ICTP RegCM3 and RegCNET. Bull. Am. Meteorol. Soc. 88, 1395–1409.
Pal, J.S., Small, E.E., Eltahir, E.A., 2000. Simulation of regional-scale water and energy budgets: representation of subgrid cloud and precipitation processes within RegCM. J. Geophys. Res. Atmos. (1984–2012) 105 (D24), 29579–29594.
Pandžić, K., Likso, T., 2005. Eastern adriatic typical wind field patterns and large-scale atmospheric conditions. Int. J. Climatol. 25, 81–98.
Papadopoulos, A., Katsafados, P., Kallos, G., Nickovic, S., 2002. The weather forecasting system for poseidon—an overview. Glob. Atmos. Ocean Syst. 8 (2-3), 219–237.
Pirazzoli, P.A., Tomasin, A., 2002. Recent evolution of surge-related events in the northern adriatic area. J. Coastal Res. 18 (3), 537–554.
Raicich, F., Pinardi, N., Navarra, A., 2003. Teleconnections between indian monsoon and sahel rainfall and the mediterranean. Int. J. Climatol. 23 (2), 173–186.
Seth, A., Rauscher, S.A., Camargo, S.J., Qian, J.H., Pal, J.S., 2007. RegCM3 regional climatologies for South America using reanalysis and ECHAM global model driving fields. Clim. Dyn. 28 (5), 461–480.
Šepić, J., Vilibic, I., Jordà, G., Marcos, M., 2012. Mediterranean sea level forced by atmospheric pressure and wind: variability of the present climate and future projections for several period bands. Glob. Planet. Change 86-87, 20–30.
Smith, S.D., Banke, E.G., 1975. Variation of the sea surface drag coefficient with wind speed. Q. J. R. Meteorol. Soc. 101 (429), 665–673.
Somot, S., Sevault, F., Déqué, M., Crépon, M., 2008. 21st century climate change scenario for the Mediterranean using a coupled atmosphere–ocean regional climate model. Glob. Planet. Change 63 (2), 112–126.
Sylla, M.B., Coppola, E., Mariotti, L., Giorgi, F., Ruti, P.M., Dell'Aquila, A., Bi, X., 2010. Multiyear simulation of the african climate using a regional climate model (RegCM3) with the high resolution ERA-interim reanalysis. Clim. Dyn. 35 (1), 231–247.
I. Tegoulias, CH. Anagnostopoulou, K. Tolika, K. Velikou, C.H. Vagenas, 2013. Effects of regional climate model spatial resolution on 10m wind field over the Aegean Sea. 13th EMS/11th ECAM, vol. 10, EMS2013-642.
Torma, C., Coppola, E., Giorgi, F., Bartholy, J., Pongráácz, R., 2011. Validation of a high-resolution version of the regional climate model RegCM3 over the carpathian basin. J. Hydrometeorol. 12 (1) doi:http://dx.doi.org/10.1175/2010JHM1234.1.
Trifonova, E., Valchev, N., Krestenitis, Y., Androulidakis, I., Kombiadou, K., Eftimova, P., Andreeva, N., Kotsev, I., Kirilova, D., 2012. Estimation of storm flood under conditions of future climate for Varna region (western Black Sea). Proceeding of 11th International Conference on Marine Sciences and Technologies—Black Sea' 2012, Varna, Bulgaria, pp. 85–91.
Trigo, I.F., Davies, T.D., Bigg, G.R., 1999. Objective climatology of cyclones in the mediterranean region. J. Clim. 12, 1685–1696.
Tsimplis, M.N., Shaw, A.G.P., 2010. Seasonal sea level extremes in the mediterranean sea and at the atlantic european coasts. Nat. Hazard Earth Syst. Sci. 10 (7), 1457–1475.

Tsimplis, M.N., Marcos, M., Somot, S., 2008. 21st century mediterranean sea level rise: steric and atmospheric pressure contributions from a regional model. Glob. Planet. Change 63 (2–3), 105–111.
Tsimplis, M.N., Marcos, M., Pérez, B., Challenor, P., Garcia-Fernandez, M.J., Raicich, F., 2009a. On the effect of the sampling frequency of sea level measurements on return period estimate of extremes—southern European examples. Cont. Shelf Res. 29 (18), 2214–2221.
Tsimplis, M., Marcos, M., Colin, J., Somot, S., Pascual, A., Shaw, A.G.P., 2009b. Sea level variability in the mediterranean sea during the 1990 on the basis of two 2D and one 3D model. J. Mar. Syst. 78 (1), 109–123.
Tsimplis, M.N., Blackman, D., 1997. Extreme sea-level distribution and return periods in the aegean and ionian seas. Estuar. Coastal. Shelf Sci. 44 (1), 79–89.
Vagenas, C., Anagnostopoulou, C., Tolika, K., 2014. Climatic study of the surface wind field and extreme winds over the Greek seas. 12th COMECAP 3 283–288.
Velikou, K., Tolika, K., Anagnostopoulou, I., Vagenas, C., 2014. High resolution climate over Greece: assessment and future projections. 12th COMECAP 3 307–312.
Villatoro, M., Silva, R., Méndez, F.J., Zanuttigh, B., Pan, S., Trifonova, E., Eftimova, P., 2014. An approach to assess flooding and erosion risk for open beaches in a changing climate. Coastal Eng. 87, 50–76.
Vilibic, I., 2000. A climatological study of the uninodal free oscillation in the adriatic sea. Acta Adriat. 41.2, 89–101.
Wang, X.H., 2002. Tide-induced sediment resuspension and the bottom boundary layer in an idealized estuary. J. Phys. Oceanogr. 32, 3113–3131.
White, A.U., 1974. Global summary of human response to natural hazards: tropical cyclones. Natural Hazards: Local, National, Global. Oxford University Press, New York, pp. 255–265.